

## Accounts

---

# Construction and Control of Self-Assembly of Amyloid and Fibrous Peptides

Hisakazu Mihara,\* Sachiko Matsumura,<sup>1</sup> and Tsuyoshi Takahashi

Department of Bioengineering, Graduate School of Bioscience and Biotechnology, Tokyo Institute of Technology, 4259-B-40 Nagatsuta-cho, Midori-ku, Yokohama 226-8501

<sup>1</sup>Corporate Research Laboratory, Corporate Research Group, Fuji Xerox Co., Ltd., 430 Sakai, Nakai-machi, Ashigarakami-gun, Kanagawa 259-0157

Received October 8, 2004; E-mail: hmihara@bio.titech.ac.jp

The aggregation of peptides and proteins into amyloid fibrils is most commonly associated with a variety of serious diseases such as Alzheimer's disease and the transmissible spongiform encephalopathies (prion diseases). Amyloid-like fibrils are undesirable states for proteins as biomolecules, however, these are fascinating nanoconstructs because of their highly ordered tertiary structure in which numerous  $\beta$ -stranded polypeptide chains align regularly. These kinds of fibrous peptides have the potential to be engineered into ones revealing basic insights into amyloid formation and protein folding, as well as developing novel peptidyl nanoscale materials. We have demonstrated that de novo designed peptides undergo self-initiated structural transition and fibril formation, showing representative properties of amyloid. Cofibril formation from two, three, or four peptide species with well-designed amino acid sequences was achieved, so that the charged residues within the  $\beta$ -strands were complementary to each other. This homologous recognition mechanism can be applied for the inhibition of the fibril formation. Meanwhile, cofibril formation indicates a possibility of functionalizing the fibrils by co-assembling of peptides with various elements to develop a fibrous peptide material as a well-ordered nanoconstruct. Another designing approach demonstrated the production of unique straight nanofibers with defined widths. The fibrils may make a nanoscaffold onto which a variety of functional groups can be arranged. The studies on engineering fibrous peptides will afford insight into disease-related amyloid formation and will help to develop nanoscale fibrous constructs.

Intermolecular self-assembly of a large number of polypeptide chains into macromolecular constructs occurs widely in biological systems. One such macromolecular self-assemblage of great interest is the amyloid fibril (Fig. 1).<sup>1–17</sup> The amyloid fibril is a misfolded and undesirable state for proteins as biomolecules, since it has been proposed to be a causative agent for a variety of fatal diseases known as amyloid diseases, such as Alzheimer's disease and prion diseases.<sup>5–8</sup> The fibril formation of peptides and proteins has attracted the attention of both the medical and the engineering communities. Improved understanding of protein misfolding is critical to the study of proteins involved in the diseases, as well as to the clarification of the folding pathway of proteins. The pathway of protein misfolding involves a conformational transition, such as that from  $\alpha$ -helix to  $\beta$ -sheet (Fig. 1).<sup>15–25</sup> This transition is especially apparent in the transformation of the  $\alpha$ -helix-rich cellular form of the prion protein (PrP<sup>C</sup>) to the scrapie isoform with higher  $\beta$ -sheet content (PrP<sup>Sc</sup>).<sup>7,8,24,25</sup>

On the other hand, the amyloid fibril has a highly ordered tertiary structure, in which numerous  $\beta$ -stranded polypeptide chains align regularly,<sup>9–12,26–28</sup> and there are therefore promis-

ing prospects for the application of this macromolecular construct in the use of proteinous materials.<sup>29–39</sup> Amyloid fibrils of misfolded natural proteins primarily comprise a single polypeptide species, a homogeneous self-assemblage. It is of great value to establish a method of fabricating and engineering fibrous peptides for the advancement of the creation of novel biomaterials. Simplified engineered peptides designed by the de novo strategy can provide useful information for constructing and manipulating peptide conformations,<sup>40–42</sup> and elucidating complex folding and misfolding mechanisms. Peptides designed for  $\beta$ -sheet folding have been studied and the subsequent formation of fibrils has been characterized.<sup>43–56</sup> A variety of designed peptides have been characterized as fibrillogenic ones, and their applications to molecular materials have been attempted in the fields of cell and tissue engineering and bionanomaterials.<sup>34–36,49,57,58</sup>

Thus, many fibrous peptides and proteins including both natural and artificial ones have been investigated. In this account, we describe our designs of amyloid and fibrous peptides and discuss the control of the formation and morphology. We have demonstrated that de novo designed peptides undergo

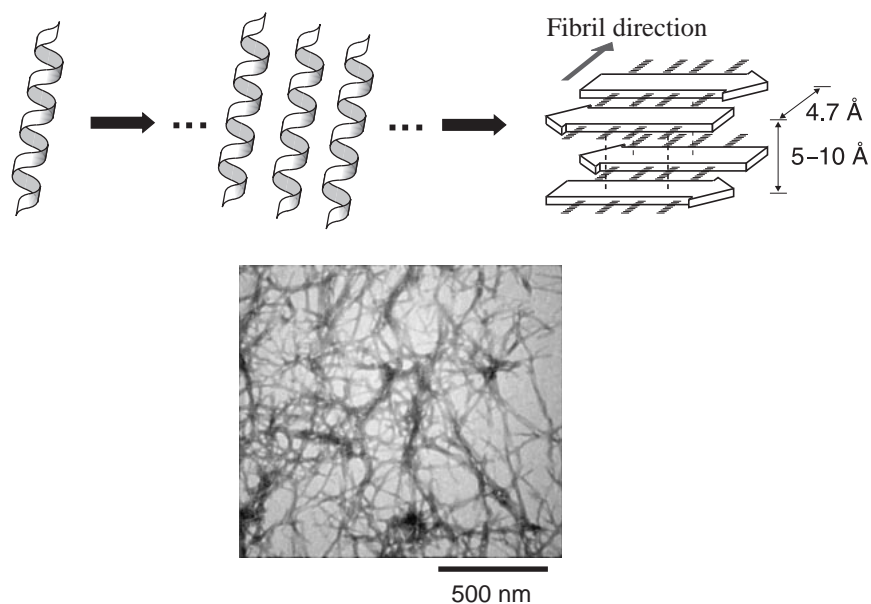


Fig. 1. Structural transition of peptide from  $\alpha$ -helix to aggregated  $\beta$ -sheet (amyloid fibril; cross  $\beta$ -structure). An example of amyloid fibrils is shown; transmission electron micrograph (TEM) of Alzheimer's amyloid  $\beta$ -peptide (1–40).

self-initiated structural transition and fibril formation, showing representative properties of amyloid.<sup>59–68</sup> Cofibril formation from two, three, or four peptide species with well-designed amino acid sequences was achieved, so that the charged residues within the  $\beta$ -strands were complementary to each other.<sup>63,64</sup> This homologous recognition mechanism can be applied for the inhibition of the fibril formation.<sup>66</sup> Meanwhile, cofibril formation indicates a possibility of functionalizing the fibrils by co-assembling of peptides with various elements to develop a fibrillar peptide material as a well-ordered nanoconstruct.<sup>67</sup> Another unique designing approach demonstrated the production of straight nanofibers with defined morphology.<sup>68</sup> The fibrils may make a nanoscaffold onto which a variety of functional groups can be arranged. The studies on engineering fibrous peptides will afford insight into disease-related amyloid formation and also will help to develop nanoscale fibrous constructs.

## 1. Design of $\alpha$ -to- $\beta$ Transitional and Fibril Forming Peptides

**1.1 Design.** A number of studies on disease-related proteins, such as those involved in Alzheimer's or the prion diseases, have led to recent improvements in our understanding of protein misfolding. The misfolding of proteins often causes a protein aggregation, initiating the fibril formation seen in  $\beta$ -amyloid peptides, prion proteins, and other amyloidogenic proteins. It is necessary to study the nature of the proteins in order to understand such critical diseases. The pathway of protein misfolding involves a conformational transition, for example, from  $\alpha$ -helix to  $\beta$ -sheet (Fig. 1).<sup>15–25</sup> This transition is especially apparent in the transformation of the  $\alpha$ -helix-rich cellular form of the prion protein (PrP<sup>C</sup>) to the scrapie isoform with higher  $\beta$ -sheet content (PrP<sup>Sc</sup>).<sup>7,8,24,25</sup> Similarly,  $\beta$ -amyloid peptides composed of 40–42 amino acid residues, which have some  $\alpha$ -helical propensity in solution, are also transformed to the amyloid form with a cross- $\beta$ -sheet structure.<sup>20</sup> In general,

one cause of protein misfolding and transformation is thought to be the exposure of the hydrophobic region of proteins in an unstable form to water environments, and the formation of aggregates that follows.<sup>10–17</sup> On the other hand, similar  $\alpha$ -to- $\beta$  transitions also occur through the correct-folding pathway in proteins with a non-hierarchical mechanism, such as  $\beta$ -lactoglobulin.<sup>21,22</sup> Moreover, the short peptide sequence named “chameleon” has been shown to adapt either an  $\alpha$ -helix or a  $\beta$ -strand at a different position in the same protein.<sup>23</sup> These behaviors suggest that the key feature in the  $\alpha$ - $\beta$  transition is the conversion from short-range interactions between nearby amino acid residues stabilizing an  $\alpha$ -helix structure to long-range interactions between secondary structures stabilizing a  $\beta$ -sheet structure.<sup>21,22</sup> That is, the structural transition is very much related to aggregation/association of peptide segments.

We have found that a hydrophobic nucleation domain, i.e., a hydrophobic defect, caused a structural transition of a peptide from an  $\alpha$ -helix to a  $\beta$ -sheet structure. We here describe the design of model peptides that undergo a self-initiated and spontaneous  $\alpha$ -to- $\beta$  transition and self-assemble into amyloid fibrils in a neutral aqueous solution (Fig. 2).<sup>59–62</sup> The designed peptide would give insight in an  $\alpha$ -to- $\beta$  transition and fibril formation of peptides and proteins.

A series of these peptides are composed of two amphiphilic  $\alpha$ -helices with double-heptad repeats (ALEQKLA)<sub>2</sub>. The two peptide chains are linked by a disulfide bond between Cys residues at the C-termini. Although an ideal amphiphilic  $\alpha$ -helix has been designed, the sequence created also has the potential to form an amphiphilic  $\beta$ -strand<sup>40,41</sup> in which hydrophobic residues and charged residues are separated on different faces of each heptad and such amphiphilicity is inverted at the center of each segment. A 1-adamantanecarbonyl (Ad) group as a hydrophobic domain is attached to the N-terminus of the peptide and is thus exposed to the solvent, which then caused intermolecular peptide associations through hydrophobic interactions.<sup>59</sup> The adamantane group was selected as the hydropho-

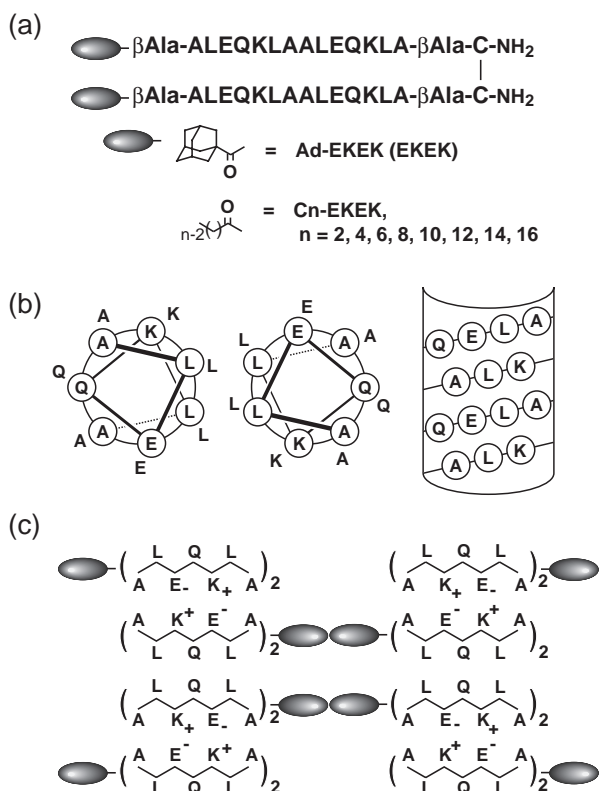


Fig. 2. Designed structure of the peptides. (a) Primary structure of the peptides with a 1-adamantanecarbonyl (Ad) group or aliphatic acyl groups (Cn) at the N-terminal. (b) A helix wheel drawing as a coiled-coil form and a net drawing of the core 14-residue peptide. (c) Schematic representation of associated  $\beta$ -structures of the core 14-peptide with hydrophobic moiety.

bic domain so that  $\beta$ -cyclodextrin could prevent the  $\alpha$ -to- $\beta$  structural transition by complexation.<sup>69–71</sup> Peptides with an acyl group in a variety of lengths (C2–C16) at the N-terminus are examined to know the effect of the hydrophobic moiety.<sup>60</sup> The 17-peptide was synthesized by the solid-phase method using 9-fluorenylmethoxycarbonyl (Fmoc) chemistry.<sup>72</sup> The dimeric peptide was synthesized via the disulfide linkage between Cys residues at the 17th position.

**1.2  $\alpha$ -to- $\beta$  Structural Transition.** The structural transition of peptides can be examined by circular dichroism (CD) measurements. The EKEK peptide (10  $\mu$ M) showed a CD spectrum typical for an  $\alpha$ -helix structure shortly after dilution in a buffer (pH 7.4) from the 2,2,2-trifluoroethanol (TFE) solution (Fig. 3). Observation of the CD spectrum revealed a gradual change to a spectrum typical for a  $\beta$ -structure, with a single negative maximum at 218 nm and a positive maximum at 198 nm after 4 h at 25  $^{\circ}$ C. The time course of the structural transition was quite sigmoidal, that is, after the lag time (ca. 90 min) the  $\alpha$ -helix conformation was rapidly transformed to the  $\beta$ -structure. The slow and autocatalytic shape of the transition bore a resemblance to the shapes of the fibril formation of natural amyloid peptides.<sup>4</sup> The autocatalytic pathway of the transition was also suggested by the observation that the transition was accelerated by seeding of a small amount (5%) of pre-formed  $\beta$ -structural EKEK, resulting in the elimination of the lag time. Fourier-transform infrared (FTIR) measurements also confirmed the  $\alpha$ -to- $\beta$  structural transition of EKEK.

**1.3 Amyloid Fibril Formation.** To characterize the aggregated and amyloid structure of the peptide, a transmission electron microscopy (TEM) experiment was employed. EKEK which was in a  $\beta$ -form (8 h after dilution at 25  $^{\circ}$ C) was absorbed onto a carbon-coated copper grid and negatively stained with uranyl acetate. TEM studies clearly showed that the  $\beta$ -structural EKEK formed a fibrillar structure (Fig. 4). The fibrils were  $\sim$ 10 nm in width and of indeterminable length (several hundreds nanometers to several micrometers), and aggregated into dense bundles. The morphology of the fibrils formed

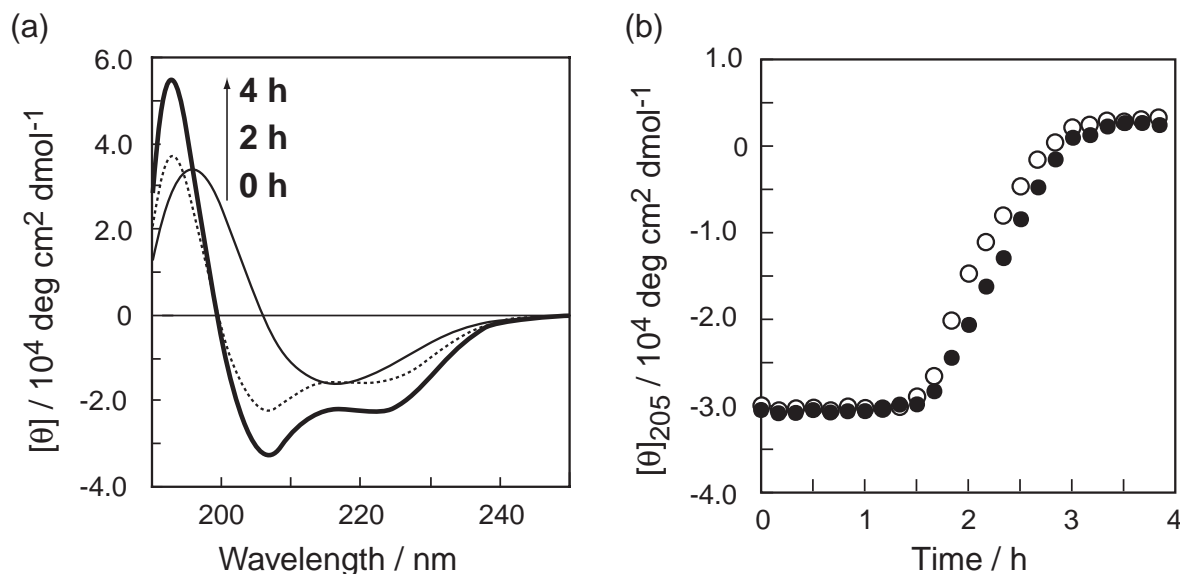


Fig. 3. CD studies of the designed peptides. CD spectral changes of Ad-EKEK (a) and time course of changes in the molar ellipticity at 205 nm of Ad-EKEK (closed circle) and C8-EKEK (open circle) (b).

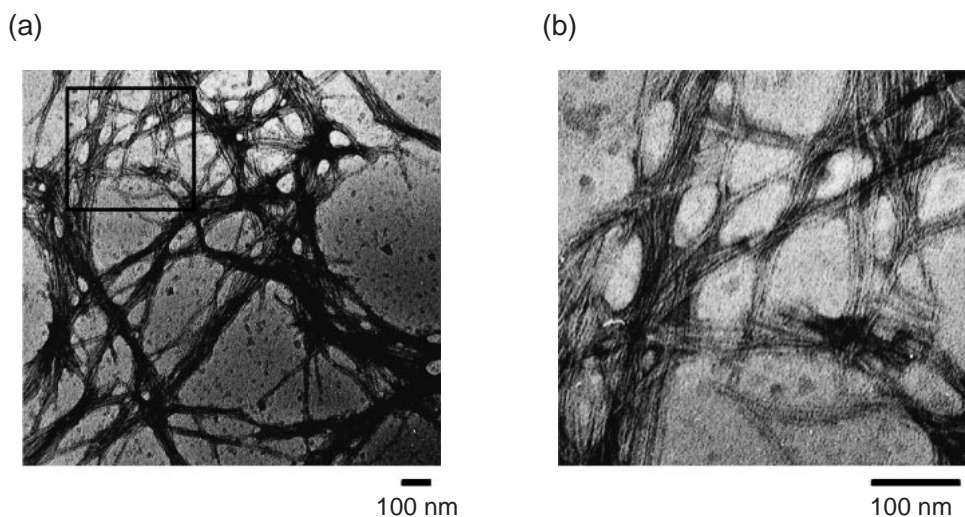


Fig. 4. TEM of Ad-EKEK in the  $\beta$ -sheet. The sample was absorbed to the grid, and then negatively stained with 2% aqueous uranyl acetate. The boxed area in (a) is magnified as (b).

by EKEK is comparable to that produced by naturally-occurring amyloid proteins and peptides, such as  $\beta$ -amyloid peptides and prion proteins.<sup>9–12,26–28</sup>

The amyloid formation of EKEK was also examined by amyloid-specific dye binding analyses using thioflavin T (ThT) and Congo Red (CR). The fluorescent dye, ThT, associates with aggregated  $\beta$ -sheet fibrils, and that binding gives rise to a significant enhancement in fluorescence according to the amount of amyloid.<sup>73</sup> ThT showed a new excitation maximum at 435 nm and an enormously enhanced emission at 482 nm.

To monitor the amyloid formation process of the peptide, we added ThT to the EKEK solution after various incubation periods (Fig. 5). The time course of fluorescence intensity at 482 nm was superimposed on that of ellipticity at 205 nm, which corresponded to the secondary structure transition, suggesting that the amyloidogenesis occurred coincidentally with the  $\alpha$ -to- $\beta$  structural transition. After the peptide took the  $\beta$ -sheet, no significant enhancements in ThT emission were observed. These results indicate that the peptides transformed to a  $\beta$ -structure assemble simultaneously into amyloid fibrils and that the amyloid formation almost completes during the secondary structure transitional process.

CR is a sulfonated azo dye which binds preferentially to protein, adopting a cross- $\beta$ -structure (Fig. 6).<sup>74</sup> When EKEK transformed to a  $\beta$ -sheet was added, CR showed an absorption spectrum characteristic for that of CR bound to a cross- $\beta$ -sheet amyloid fibril, which exhibits double maxima at approximately 514 nm and 530 nm. This result indicates that  $\beta$ -structural EKEK assembles into a regular tertiary structure consistent with a cross- $\beta$ -sheet structure.

**1.4 Effect of Hydrophobic Group.** It became clear that N-terminal acyl groups of particular lengths such as Ad in a  $2\alpha$ -helix peptide (EKEK) caused the peptide to undergo an  $\alpha$ -to- $\beta$  transition.<sup>59</sup> Among the acyl-chained  $2\alpha$ -peptides ranging from C2 to C16, the octanoyl C8 group was the most effective for inducing the  $\alpha$ -to- $\beta$  transition (Fig. 7).<sup>60</sup> Using the octanoyl group provided optimum hydrophobicity for the conformational defects. The peptides with lower hydrophobicity than C6 (C2- and C4-EKEK) showed a lower  $\alpha$ -helix propensity, but

did not completely transform to a  $\beta$ -structure. The peptides with higher hydrophobicity than C10 (C12- to C16-EKEK) formed stable  $\alpha$ -helix oligomers, but did not transform to a  $\beta$ -structure. The  $2\alpha$ -peptides with longer acyl chains (C12- to C16-EKEK) formed more stable  $\alpha$ -helices than C8-EKEK due to the formation of oligomers in the initial  $\alpha$ -helix state. The transitional peptides (C6-, C8-, and C10-EKEK) were in a monomeric state at the initial stage and then aggregated to  $\beta$ -sheets, forming fibrous structures.

This study using the acyl chains, in addition to the previous work with Ad-group, suggests that unstable  $\alpha$ -helix aggregates (oligomer or larger) are an intermediate (first nucleus) of the structural transition (Fig. 8). Based on this assumption, the conformation of a peptide with moderate hydrophobicity, such as that of Ad-EKEK or C8-EKEK, would exist in an equilibrium between monomers and aggregates in  $\alpha$ -helix. When a critical amount of  $\alpha$ -helix aggregates accumulate, which gives rise to new long-range (intermolecular) interactions, the peptide conformation transforms to  $\beta$ -sheet in an autocatalytic manner. The time necessary for the accumulation of  $\alpha$ -helix aggregates may correspond to the lag time for nucleation,<sup>4</sup> although the  $\alpha$ -helix aggregates are so unstable that they cannot be easily detected by a method such as size-exclusion chromatography. Once the  $\beta$ -aggregates appear, monomeric or oligomeric  $\alpha$ -helix species could further transform to the  $\beta$ -sheet on the template aggregates. In contrast, when a peptide forms stable  $\alpha$ -helix oligomers such as C12- to C16-EKEK, the conformation of the peptide is not transformed. A peptide with a less hydrophobic domain, such as C2-EKEK, remains stable as a monomeric  $2\alpha$ -helix and cannot form an  $\alpha$ -helix nucleus, thus it cannot acquire the long-range interaction which would stabilize the  $\beta$ -structure. Therefore, there appears to be an optimum length for the hydrophobic domains.

One role of the hydrophobic domain would thus be the formation of an  $\alpha$ -helix nucleus. In other words, the hydrophobic clustering by the conformational defects may form unstable  $\alpha$ -helix aggregates, which would then initiate the cooperative conversion from short-range interactions to long-range interactions, thereby triggering the autocatalytic transition to  $\beta$ -sheet

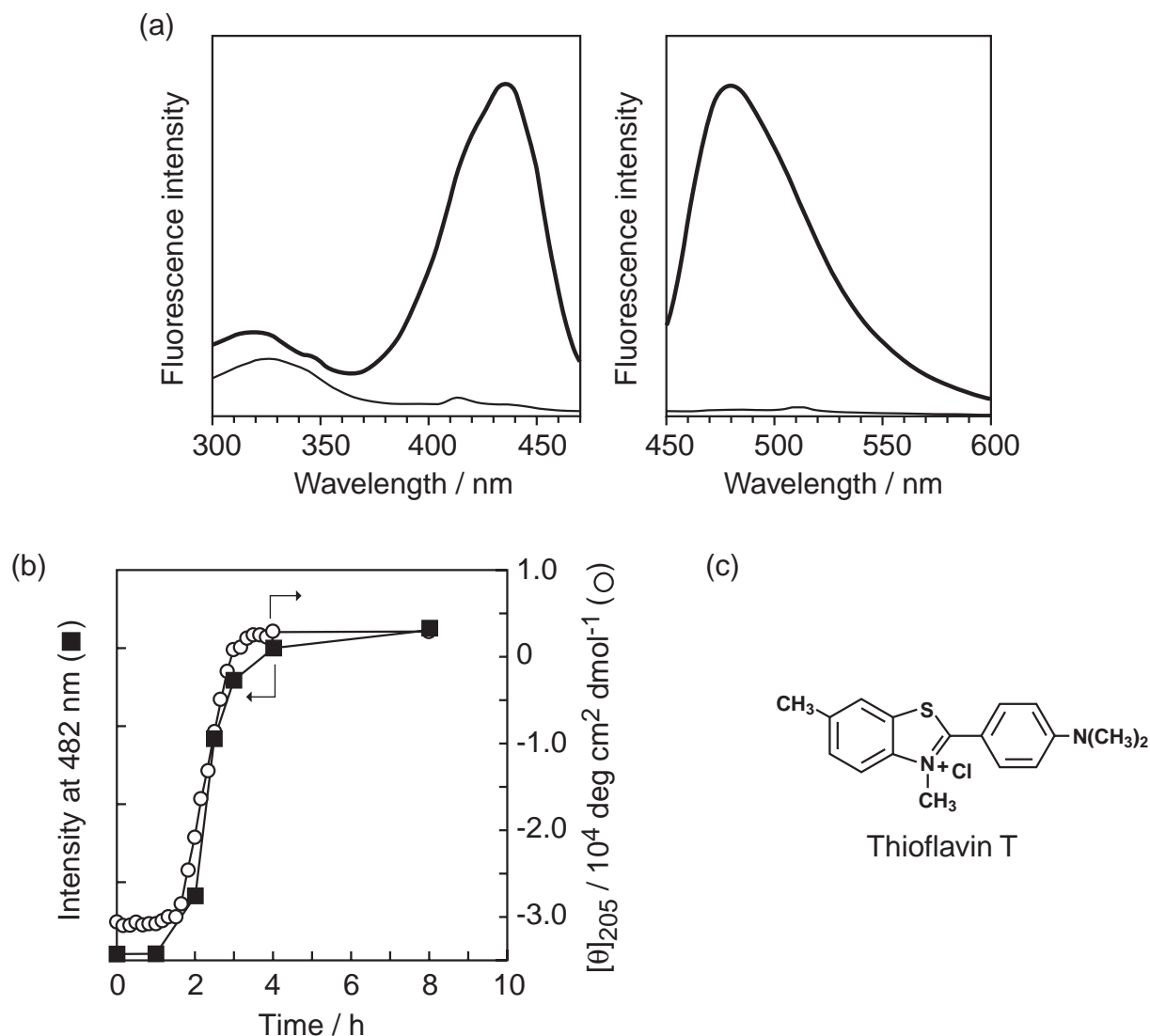


Fig. 5. Thioflavin T (ThT) binding analysis. (a) Excitation spectra (left) and emission spectra (right) of ThT in the presence of Ad-EKEK in  $\alpha$ -helix (0 h) (thin line) or  $\beta$ -sheet (8 h) (bold line).  $\lambda_{em} = 482$  nm (left) and  $\lambda_{ex} = 435$  nm (right). (b) Time course of ThT fluorescence intensity at 482 nm (closed square) in the presence of Ad-EKEK and the molar ellipticity at 205 nm of Ad-EKEK (open circle). [Ad-EKEK] = 10  $\mu$ M and [ThT] = 6  $\mu$ M in 20 mM Tris-HCl buffer (pH 7.4)/2.5% TFE at 25  $^{\circ}$ C. (c) Structure of ThT is indicated.

conformation. The two-segmental peptide is designed to form either an amphiphilic  $\alpha$ -helix or an amphiphilic  $\beta$ -sheet using Leu residues for the hydrophobic core (Fig. 2), indicating that it has a chameleon property.<sup>23</sup> The conformation of such a de novo designed peptide has been characterized as a molten-globule-like structure.<sup>42</sup> Although the mechanism of the  $\alpha$ -to- $\beta$  transition step is certainly more complex and will require further clarification, it is plausible that the formation of unstable  $\alpha$ -helix aggregates like a molten-globule-like structure occurs during the lag time and is the rate-determining step and, therefore, that the initial  $\alpha$ -helix structure and its stability are significant determinants for the transition. It has also been suggested that the formation of relatively unstable intermediates of proteins in folding pathways or by unfavorable mutations triggers the aggregation and structural transition.<sup>13–17</sup> Especially in the prion proteins, it has been proposed that the transformation from an  $\alpha$ -helix to a  $\beta$ -sheet structure induces

the formation of aggregates as a seed for amyloidogenesis.<sup>7,8,25</sup> The formation of  $\alpha$ -helix structure seems to be important in the transition kinetics, because the transition of peptides with an almost random conformation takes much longer time and/or needs higher temperature and concentration than that of peptides with an  $\alpha$ -helix structure. The initiation of  $\alpha$ -to- $\beta$  transition by introducing hydrophobic domains may provide insight into the conformational changing process that has been widely observed in protein research. The design concept employed here could potentially lead to a model system for controlling self-assembly of polypeptides, which will also lead to the development of peptidyl self-assembling materials.

**1.5 Effects of Cyclodextrin, Organic Solvent, Temperature, pH, and Detergent.** It is well known that  $\beta$ -cyclodextrin ( $\beta$ CDx) strongly captures an adamantane derivative into the hydrophobic cavity.<sup>69–71</sup> Therefore,  $\beta$ CDx was expected to prevent the peptide aggregation by capturing the exposed



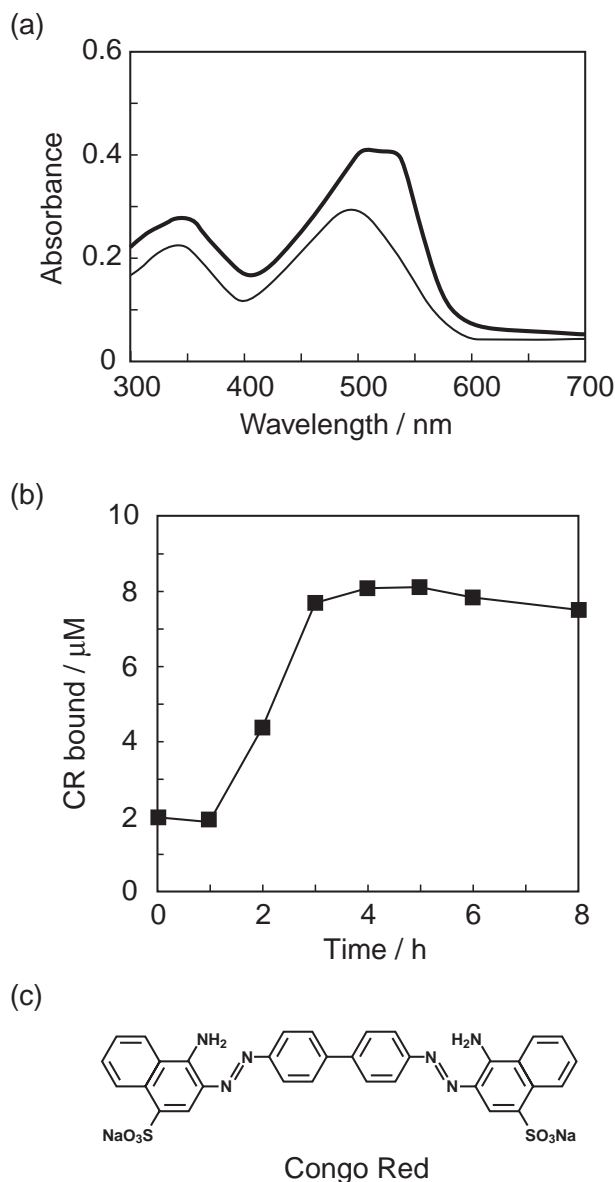


Fig. 6. Congo Red (CR) binding analysis. (a) Absorption spectra of CR in the presence of Ad-EKEK incubated for 0 h (thin line) or 8 h (bold line) in the buffer at 25 °C. (b) Time course of the amount of CR bound to the  $\beta$ -sheet fibrils formed by Ad-EKEK. [Ad-EKEK] = 9  $\mu$ M and [CR] = 10  $\mu$ M. (c) Structure of CR is indicated.

Ad group within the cavity (Fig. 9). The addition of  $\beta$ CDx to the solution of peptide EKEK while it was in the  $\alpha$ -helical state retarded the  $\alpha$ -to- $\beta$  transition with increasing concentration of  $\beta$ CDx. The addition of 10 equiv. of  $\beta$ CDx to the Ad group completely inhibited the transition. Size-exclusion chromatography revealed that the association of peptides did not take place in the presence of  $\beta$ CDx. The prevention of the aggregation with  $\beta$ CDx inhibited the structural transition. The Ad groups are defects in the  $\alpha$ -helix peptide and nucleate the peptide aggregation, which subsequently causes the structural transition.

The increasing temperature accelerated the structural transition, and chilling decreased the transitional rate. The tempera-

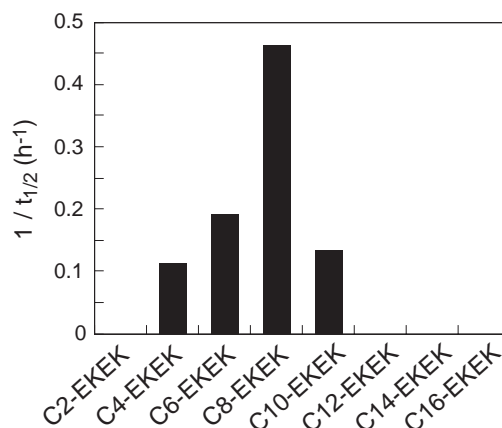


Fig. 7. Transitional rate ( $1/t_{1/2}$ ) to  $\beta$ -sheet of C<sub>n</sub>-EKEK peptides with various acyl chains. The data were evaluated by changes in the molar ellipticity of CD at 205 nm. C2 and C12–16 are non-transitional peptides.

ture-dependence of the reaction supports the idea that hydrophobic interactions are responsible for the aggregation and the transition. The lag time was proportional to  $t_{1/2}$  of the  $\alpha$ -to- $\beta$  transition curve, indicating that the lag time is essential for the transition. The lag times are considered to be necessary for the nucleation of the amyloid formation.<sup>4</sup>

The structural transition of EKEK was dependent on the concentration of peptide. The  $\alpha$ -to- $\beta$  transition occurred at the concentration of 2  $\mu$ M. Increases of peptide concentration of up to 10  $\mu$ M linearly enhanced the transition rate with shortening the lag time period for  $\beta$ -sheet formation. This concentration dependence supports the above assumptions that the lag time is essential to the structural transition and that the aggregation process coincides with the reaction. Further increasing the concentration to more than 20  $\mu$ M prevented the analyses due to the rapid formation of insoluble materials.

As shown in the illustration of the peptide as a  $\beta$ -form (Fig. 2), the hydrophobic Leu residues and hydrophilic Glu and Lys residues are separated to form a kind of amphiphilic  $\beta$ -structure. The hydrophobic interactions between Leu residues and the electrostatic interactions between Glu and Lys residues contribute to the structural transition. Therefore, the addition of an organic solvent TFE and detergents should affect the transition of EKEK. Salt and pH were also effective. The addition of TFE to weaken the hydrophobic interaction between Ad groups or Leu residues decreased the transitional rate linearly with increasing content of TFE. When more than 5% TFE was added, the transition did not occur and the peptide remained as a monomer.

The highest transition rate took place at neutral pH, but the rate was retarded by changing to acidic or basic pH. At pH 3, the structural transition did not take place and the peptide was monomeric on the size-exclusion column. At pH 9, the transition rate was one-third of that at neutral pH. The addition of NaCl also retarded the structural transition in a concentration-dependent manner, the rate with 1 M NaCl being one-third of that without the salt. These pH and salt effects suggested that the electrostatic interactions also contribute, along with the hydrophobic interactions, to the  $\alpha$ -to- $\beta$  transition. Furthermore, the inhibition experiments, in which  $\beta$ CDx or TFE was

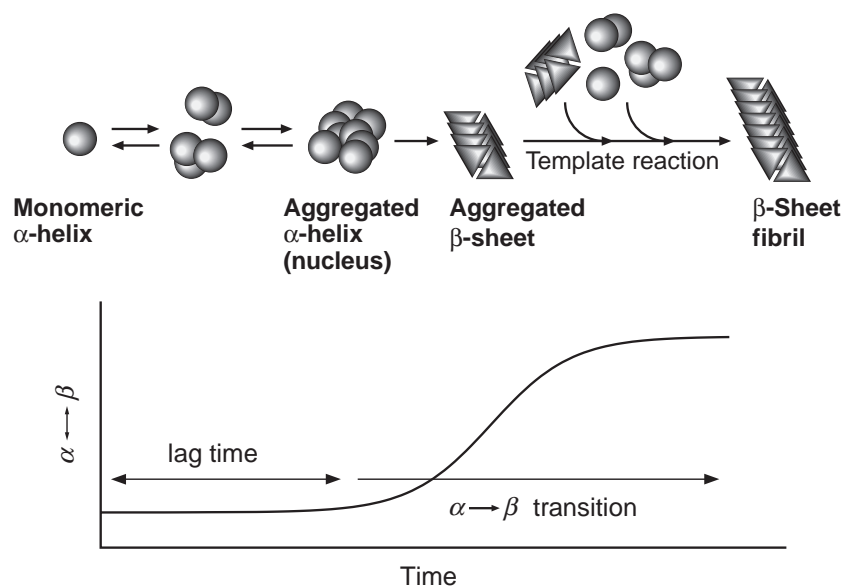


Fig. 8. A proposed mechanism of the  $\alpha$ -to- $\beta$  structural transition. In the initial stage, the peptide with a moderate hydrophobic domain, such as Ad or C8 group, exists in an equilibrium between a monomeric and oligomeric/aggregated  $\alpha$ -helix structure, although the monomeric species is dominant. A nucleation of the  $\alpha$ -helices occurs during the lag time, and the resultant long-range (intermolecular) interactions, which stabilize a  $\beta$ -sheet structure, initiate a cooperative exchange of hydrogen bonds toward the  $\beta$ -sheet conformation. Once the  $\beta$ -sheet aggregates appear, monomeric or oligomeric  $\alpha$ -helix species could further transform to  $\beta$ -sheet on the template aggregates, resulting in simultaneous fibril formation.

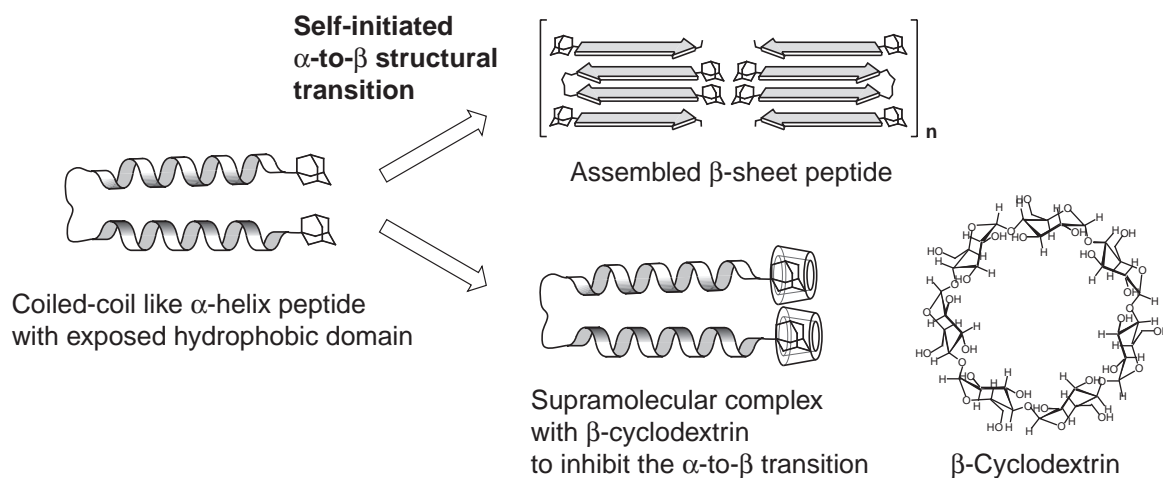


Fig. 9. Illustration of the  $\alpha$ -to- $\beta$  transition of Ad-EKEK and inhibition by  $\beta$ -cyclodextrin.

added or pH was changed, showed that prevention of the peptide aggregation inhibits the  $\alpha$ -to- $\beta$  transition, supporting the conclusion that the peptide aggregation is an important step for the transition.

A cationic detergent cetyltrimethylammonium bromide (CTAB) and an anionic detergent sodium dodecyl sulfate (SDS) similarly retarded or inhibited the structural transition of EKEK in a concentration-dependent manner. Both detergents completely inhibited the transition at concentrations over 0.5 mM. The detergents could be expected to affect the hydrophobic interactions between Ad groups and between helices, resulting in perturbation of the 3D structure. It is noteworthy that the non-ionic detergent NP-40 (polyoxyethylene(9) octylphenylether) did not influence the structural transition up to 5 mM. Perturbation of both electrostatic and hydrophobic inter-

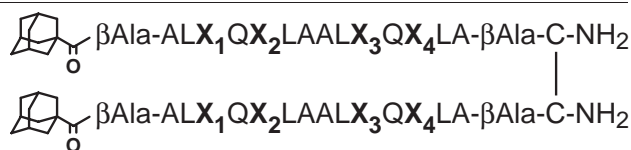
actions by the cationic and anionic detergents is effective for inhibiting the reaction.

## 2. Heterogeneous Assembly of Complementary Peptide Pairs into Amyloid Fibrils

**2.1 Design.** Intermolecular self-assembly of a large number of polypeptide chains into macromolecular constructs occurs widely in biological systems. One of such macromolecular self-assemblages of great interest is the amyloid fibril. Amyloid fibril primarily comprises a single polypeptide species, namely, it is a homogeneous self-assemblage. This may be related to species specificity in the infectious agent of a prion.<sup>7</sup> Meanwhile, heterogeneous co-assembly of designed peptides into fibrils would be beneficial to be engineered into peptidyl materials.<sup>37</sup> We have accomplished the heterogeneous

Table 1. Structure of Designed Peptides with Various Arrangements of Charged Residues

Peptide	X <sub>1</sub>	X <sub>2</sub>	X <sub>3</sub>	X <sub>4</sub>					Total charge at neutral pH
1.EEEE	E	E	E	E	—	—	—	—	−8
2.EEEK	E	E	E	K	—	—	—	+	−4
3.EEKE	E	E	K	E	—	—	+	—	−4
4.EKEE	E	K	E	E	—	+	—	—	−4
5.KEEE	K	E	E	E	+	—	—	—	−4
6.EEKK	E	E	K	K	—	—	+	+	0
7.EKEK	E	K	E	K	—	+	—	+	0
8.EKKE	E	K	K	E	—	+	+	—	0
9.KEEK	K	E	E	K	+	—	—	+	0
10.KEKE	K	E	K	E	+	—	+	—	0
11.KKEE	K	K	E	E	+	+	—	—	0
12.EKKK	E	K	K	K	—	+	+	+	+4
13.KEKK	K	E	K	K	+	—	+	+	+4
14.KKEK	K	K	E	K	+	+	—	+	+4
15.KKKE	K	K	K	E	+	+	+	—	+4
16.KKKK	K	K	K	K	+	+	+	+	+8



assembly into fibrils by complementary electrostatic interactions between pairs of peptide species; each of which is not able to self-assemble.<sup>63,64</sup>

The design of peptides that could heterogeneously assemble into amyloid fibrils commenced by engineering our de novo designed peptides that homogeneously self-assembled into fibrils. The peptides undergo a self-initiated structural transition from an  $\alpha$ -helix to a  $\beta$ -sheet in neutral aqueous solution, and simultaneously self-assemble into fibrils in an autocatalytic manner. The parent peptide was 7.EKEK in Table 1. The amino acid sequence of the original peptide contains four charged residues; two glutamic acid (negatively-charged E) residues and two lysine (positively-charged K) residues (Table 1). We manipulated these charged residues as the complementary determining residues for the peptide assembly into fibrils. To this end, we prepared all types of Ad-linked peptides bearing glutamic acid or lysine residues at positions X<sub>1</sub>–X<sub>4</sub> (Table 1). Conformational analysis of these peptides was carried out by CD spectroscopy, and fibril formation was analyzed by TEM and amyloid-specific dye ThT binding studies.

**2.2 Two Peptide Species into Fibrils.** CD studies revealed that all 16 peptides predominantly formed an  $\alpha$ -helix or a random coil structure depending on their sequences shortly after dissolution in the neutral buffer (12  $\mu\text{M}$  at 25 °C). No  $\beta$ -sheet structure was observed in the initial stage. Since intermolecular association of the peptides is required for the formation of  $\beta$ -sheet fibrils, it is expected that neutrally-charged peptides will assemble into fibrils more readily than negatively- or positively-charged peptides. The CD, TEM, and ThT-binding studies revealed that, among the six neutrally-charged peptides (6.EEKK to 11.KKEE), four peptides, 6.EEKK, 7.EKEK, 10.KEKE, and 11.KKEE, were able to self-assemble into  $\beta$ -sheet fibrils after 4 h. The other two neutrally-charged pep-

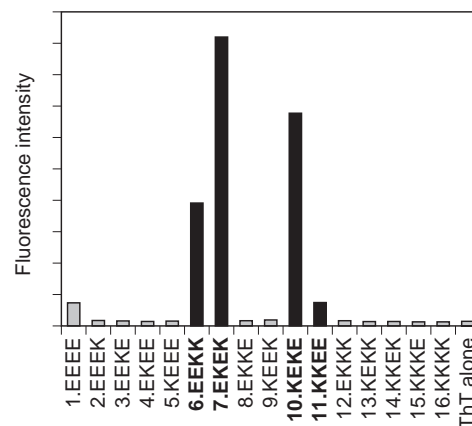


Fig. 10. Amyloid fibril formation of 16 designed peptides examined by the ThT assay. Peptides No. 6, 7, 10, and 11 are confirmed to form fibrils by TEM.

tides, 8.EKKE and 9.KEEK, were not able to form  $\beta$ -sheet fibrils even after 4 days (Fig. 10). These results suggest that the positions of positive and negative charges are critical for the well-organized assembly of  $\beta$ -strands, and that these four peptides have self-complementary sequences which enable them to homogeneously self-assemble into fibrils (discussed below). None of the negatively- (1.EEEE to 5.KEEE) or positively-charged peptides (12.EKKK to 16.KKKK) was able to form  $\beta$ -sheet fibrils (Fig. 10), which is due to their disfavored intermolecular associations.

From all possible mixing pairs of 16 peptides (total 120 combinations), we searched for complementary pairings that enabled heterogeneous co-assembly of two peptide species into amyloid fibrils.<sup>63</sup> Two species were mixed at equimolar ratios (6  $\mu\text{M}$  each) and incubated in neutral buffer for 24 h, and then fibril formation was examined by ThT-binding analysis (Fig. 11). The combinations of interest are those of negatively- and positively-charged peptides that neutralize the net charge (blue region in Fig. 11). Since none of them is able to form  $\beta$ -sheet fibrils individually (Fig. 10), co-assembly into fibrils is expected only when another peptide species coexists in the solution. From the blue region in Fig. 11, four specific pairings were selected as fibril-forming ones. The TEM study confirmed that these mixtures indeed formed the fibrillar assemblages. The CD studies revealed that each of the four selected pairs formed an  $\alpha$ -helix structure initially, and changed to a  $\beta$ -sheet structure spontaneously, whereas each species alone existed predominantly as an  $\alpha$ -helix or random coil over 4 days. In each of the four pairs, the  $\alpha$ -helicity of the mixture was higher than the values in single species solutions, suggesting that the two species interact with each other prior to  $\beta$ -sheet fibril formation. Additional fibril-forming pairing was observed in 8.EKKE/9.KEEK (Fig. 11), each of which was neutrally-charged but unable to form fibrils individually (Fig. 10).

**2.3 Three and Four Peptide Species into Fibrils.** Next, the complementary triplets (three different peptides) that heterogeneously co-assemble into the fibrils were identified from the peptide library.<sup>64</sup> In this screening, we examined mixtures of two different peptides from anionic 2.EEEK–5.KEEE together with an additional cationic peptide 16.KKKK. These



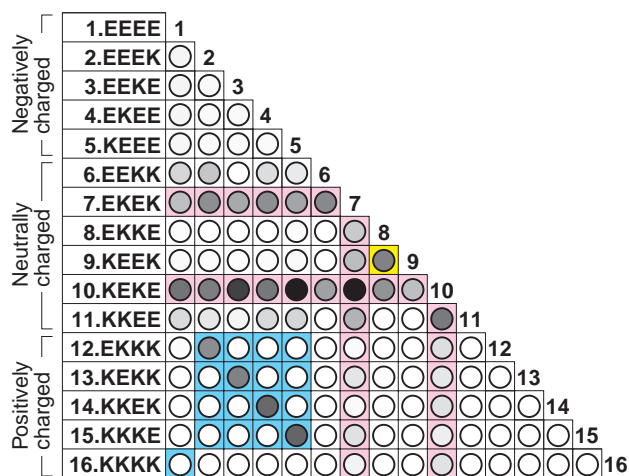


Fig. 11. Complementary peptide pairs capable of assembling heterogeneously into fibrils. Fibril formation of the two-peptide mixtures was examined by the ThT-binding analysis using a multi-well plate reader. The fluorescence intensities of ThT in the presence of the mixtures are represented by the black color density of the circles, and regions of interest are marked in blue and yellow.

combinations (two  $-4$ -peptides and one  $+8$ -peptide) were chosen for three reasons: 1) no species can form the fibrils by itself;<sup>63</sup> 2) no two pairs selected from these peptides can be the complementary pairs for the heterogeneous assembly;<sup>63</sup> and 3) the equimolar mixture of these three species neutralizes the net charge. Thus, six possible combinations of triplets were generated (Fig. 12a).

Three species were mixed at equimolar ratios (4  $\mu$ M each, total 12  $\mu$ M) and incubated in a buffer (pH 7.4) at 25  $^{\circ}$ C. The fibril formation of triplets was then examined by the ThT and TEM analyses (Fig. 12a). The results of this screening indicated that only two combinations, 2.EEEK/4.EKEE/16.KKKK and 3.EEKE/5.KEEE/16.KKKK, are fibril-forming complementary triplets. The CD study revealed that these mixtures (2.EEEK/4.EKEE/16.KKKK and 3.EEKE/5.KEEE/16.KKKK) initially form an  $\alpha$ -helix structure and then change to a  $\beta$ -sheet structure within 2 days. Furthermore, the  $\alpha$ -helicity of these three-peptide mixtures at the initial stage was higher than that of solutions containing the single species, suggesting that these species interact with each other prior to  $\beta$ -sheet fibril formation. The complementary interactions of the charged groups are also important in  $\alpha$ -helix formation at the initial stage.

Furthermore, heteroassembly of four peptide species complementarily into amyloid fibrils was also accomplished (Fig. 12b).<sup>64</sup> In identifying complementary triplets described above, the triplets 2.EEEK/3.EEKE/16.KKKK, 2.EEEK/5.KEEE/16.KKKK, 3.EEKE/4.EKEE/16.KKKK, and 4.EKEE/5.KEEE/16.KKKK were unable to assemble complementarily into the fibrils (Fig. 12a). It was thought possible that the addition of a fourth species to these non-complementary triplets might lead to the complementary assembly of four species into amyloid fibrils. 8.EKKE and 9.KEEK were chosen to be the fourth species because each is neutrally charged and is unable to form the fibrils individually. The equimolar mixture of four species including 8.EKKE or 9.KEEK results in

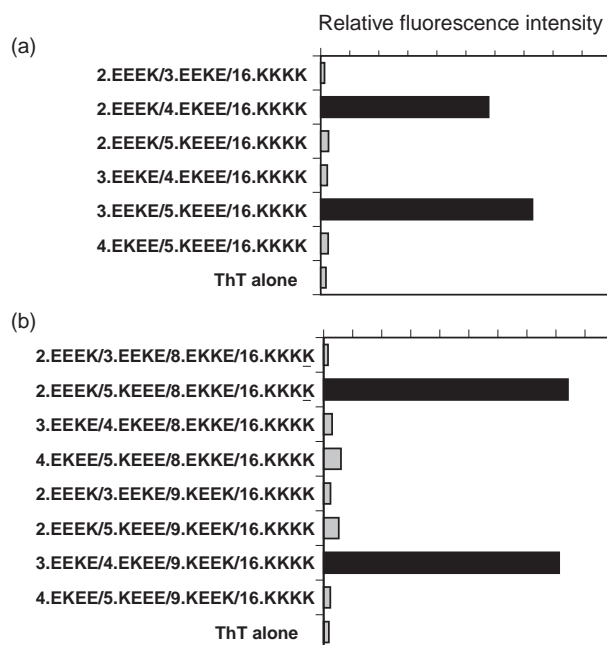


Fig. 12. Complementary peptide triplets and quadruplets capable of assembling heterogeneously into fibrils. Fibril formation of the three-peptide (a) and four-peptide (b) mixtures was examined by the ThT-binding analysis.

the neutralization of the net charges (two  $-4$ -peptides, one  $+8$ -peptide and one  $\pm 0$ -peptide). All eight combinations of quadruplets were thus generated (Fig. 12b).

The four species were mixed at equimolar ratios (3  $\mu$ M each, total 12  $\mu$ M) and incubated in the buffer for 5 days at 25  $^{\circ}$ C. The ThT-binding analysis indicated that two quadruplets, 2.EEEK/5.KEEE/8.EKKE/16.KKKK and 3.EEKE/4.EKEE/9.KEEK/16.KKKK, possess an outstanding ability to form amyloid fibrils, but the others possess little or no such ability (Fig. 12b). The TEM study revealed that the morphology of the fibrils formed by the quadruplet mixtures is essentially identical to that of fibrils formed by the complementary triplet mixtures.

**2.4 Complementary Assembly Model.** The results shown in Fig. 11 clearly demonstrate that there are complementary pairings of the peptides which enable them to assemble heterogeneously into amyloid fibrils.<sup>63</sup> From the fibril-forming two-species combinations, 2.EEEK/12.EKKK, 3.EEKE/13.KEKK, 4.EKEE/14.KKEK, 5.KEEE/15.KKKE, and 8.EKKE/9.KEEK, we observed a trend explaining why these pairings are compatible. As shown in Fig. 13, in all five cases, if the two species are aligned inversely, they are able to form complete negative-positive charge pairings. Thus, two species of  $\beta$ -strands would be arrayed in antiparallel to form ion pairs in the fibrils. This trend also illustrates why some neutrally-charged peptides are able to form fibrils homogeneously, but others are not (Fig. 10). The homogeneous fibril-forming peptides, 6.EEKK, 7.EKEK, 10.KEKE, and 11.KKEE, can form ion pairs intermolecularly if the strands are aligned in antiparallel, meaning that their sequences are self-complementary (Fig. 13).

According to the above model, a schematic representation illustrates the heterogeneous co-assembly of three or four spe-

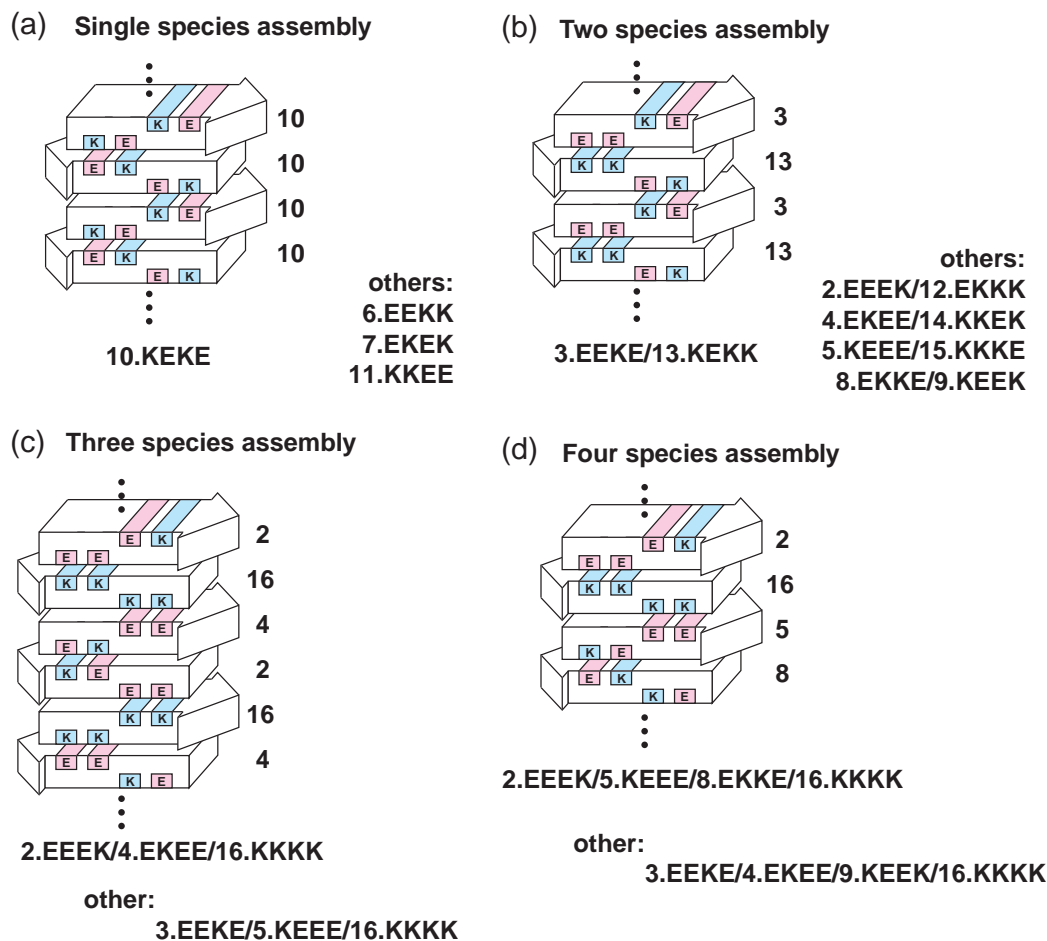


Fig. 13. Assembly models of complementary peptide singlets, doublets, triplets, and quadruplets. Complete sets of complementary charge residues are accomplished.

cies as shown in Fig. 13.<sup>64</sup> In the assembly of triplet or quadruplet peptides, an antiparallel molecular arrangement was also applied. This model of amyloid assembly is an idea combining both the complementary assembling models of the electrostatic face<sup>63</sup> and the hydrophobic face.<sup>62</sup> The model in Fig. 13 can explain why the two triplets or quadruplets are able to form amyloid fibrils among six or eight combinations of three or four peptide mixtures, respectively. In this model, both the electrostatic and hydrophobic interactions were complementarily arranged at both upper and lower faces of  $\beta$ -strands. Complete sets of matched charged residues, E and K, are accomplished only when the two triplets or quadruplets are aligned in the complementary manners.

The heterogeneous assembly into fibrils is obviously accomplished by the complementary interactions between two, three or four peptide species.<sup>62–64</sup> These models demonstrated that both the peptides homogeneously assembling into amyloid fibrils and the peptide pairs assembling heterogeneously must follow the rule of the complementary pairings of charged residues E(–) and K(+) between  $\beta$ -strands laminated into amyloid fibrils. In other word, the peptides unable to form the electrostatic pairings cannot form amyloid fibrils easily. Also, in respect to the hydrophobic face of the  $\beta$ -strand, the similar complementary pairing was found to be essential to form two-species co-assembly of analogous peptides mutated at the hy-

drophobic face.<sup>62</sup>

In these co-assembling studies, heterogeneous combinations of two, three, or four peptide species, each of which is unable to self-assemble individually, assemble complementarily into amyloid fibrils and simultaneously undergo an  $\alpha$ -to- $\beta$  structural transition. MacPhee and Dobson reported the incorporation of fluorescent labels into the fibrils by the co-assembly of two peptide species derived from natural proteins (1% w/w of a labeled peptide and an unlabeled one), where the labeled peptide is distributed irregularly in the fibril.<sup>37</sup> The results presented here are the first demonstration of an approach for constructing a heterogeneously assembled polypeptide fibril composed of multiple species, in which the alignment and orientation of each species may be highly ordered. This could be accomplished by using simplified de novo designed polypeptides. Thus, this approach will enable the site-specific incorporation of multiple kinds of functional groups or structural probes (e.g., isotopes, fluorophores, and spin labels) into this construct with the sequential array in the fibril. This is an important step toward the creation of nanoscale materials through the use of polypeptide fibrils with novel functional, physicochemical, and mechanical properties (discussed later).<sup>34–38</sup> To efficiently study the fine details of protein organization, the use of simplified model peptides like those presented here leads to a clearer understanding of underlying mechanisms whereby conforma-

tional change and the aggregation/assembly of proteins occur. Moreover, the complementary assembly of  $\beta$ -strands demonstrated here will lead to the identification of the precise molecular details of the amyloid structure which have not yet been fully resolved.<sup>9–12</sup> This strategy using homologous peptides can be also applied to design of inhibitors developed on the basis of molecular models. This topic is developed in the next section.

### 3. Inhibition of Fibril Formation by Cationic Peptides with Homologous Sequences

Conformational alternation and fibril formation of proteins have a key role in a variety of amyloid diseases including Alzheimer's and prion diseases. We have successfully developed peptides that undergo self-initiated structural transition from  $\alpha$ -helix to  $\beta$ -sheet and self-assembling into amyloid fibrils.<sup>59–65</sup> Peptides could be manipulated to assemble into amyloid fibrils in single and multiple (two, three, and four) species.<sup>59–64</sup> These studies afforded the idea that homologous sequences of peptides have key roles in the  $\beta$ -sheet assembly and amyloid formation. Generally, the amyloid peptides and proteins undergo self-assembling into fibrous structures. That is, the peptides and proteins make amyloid fibrils homogeneously, thus exhibiting the single-species recognition in amyloid transmission and amplification.<sup>1–4,9–12</sup> Taking these aspects into consideration, utilization of peptides with homologous sequences will lead to control of the conformational transition and subsequent amyloid fibril formation. An inhibition system of amyloid formation of peptides using this concept was constructed.<sup>66</sup> There have been some reports on the inhibition against aggregation of amyloid  $\beta$ -protein of Alzheimer's diseases by hydrophobic peptides homologous to the native sequence.<sup>75–78</sup> In this study, we focused on the hydrophilic regions of the model amyloid peptides, EKEK (Fig. 2). To inhibit structural transition and aggregation of the amyloidogenic peptide, the homologous peptides whose sequences were sys-

tematically substituted at charged amino acids of EKEK were employed (Table 1). It has been found that cationic peptides in the 16 peptide variants strongly prevented the structural transition and amyloid formation of EKEK. Hence, the inhibition abilities of peptides analogous to a cationic peptide KKKK were also studied. Consequently the peptides with higher homology to EKEK showed stronger inhibition abilities.<sup>66</sup>

The peptide 7.EKEK that undergoes  $\alpha$ -to- $\beta$  structural transition and amyloid fibril formation has been studied as a mother compound of amyloidogenic peptides that we used (Fig. 2 and Table 1). To find out an inhibition system of the  $\alpha$ -to- $\beta$  structural transition and amyloid formation of 7.EKEK series of fifteen homologous peptides substituted at charged amino acids of 7.EKEK were employed (Table 1).

**3.1 Inhibition of Structural Transition.** Inhibition in the structural transition of EKEK in the presence of peptides with homologous sequences was examined by CD spectroscopy.<sup>66</sup> EKEK alone underwent the structural transition from  $\alpha$ -helix to  $\beta$ -sheet when it was incubated in a buffer solution for 24 h at 25 °C (Fig. 3). By contrast, the peptide maintained the  $\alpha$ -helix structure when EKEK was incubated with the homologous peptide KKKK. The other cationic peptides (12.EKKK–15.KKKE) also inhibited the  $\alpha$ -to- $\beta$  structural transition of EKEK while neutral peptides (6.EEKK–11.KKEE) did not (Fig. 14a). Anionic peptides (2.EEEK–5.KEEE) slightly inhibited the structural transition of EKEK, but their potentials were much weaker than those of the cationic peptides. The most anionic peptide EEEE was not used in this study, because it was not highly soluble in the assay system. As a result, cationic peptides had stronger inhibition abilities for the structural transition of the amyloidogenic EKEK.

**3.2 Inhibition of Fibril Formation.** Inhibition in the amyloid formation of EKEK in the presence of the homologous peptides was then examined by the amyloid-specific dye ThT binding analysis.<sup>66</sup> EKEK was incubated with each of the homologous peptides for 24 h at 25 °C, and then fluores-

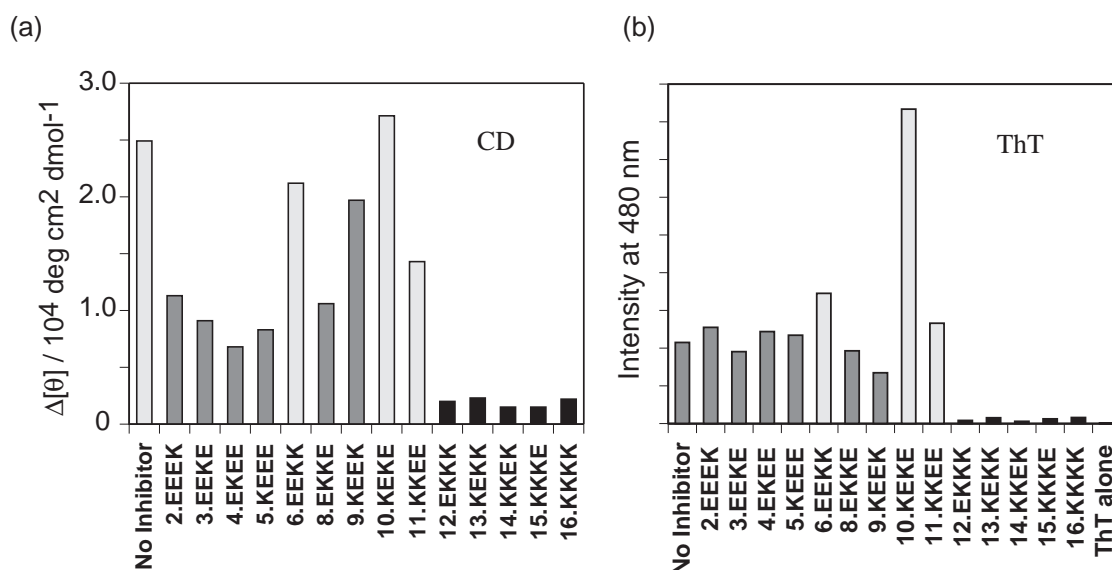


Fig. 14. Inhibition of fibril formation of EKEK by cationic peptides such as KKKK with homologous sequences with EKEK. (a) Inhibition of  $\alpha$ -to- $\beta$  structural transition examined by CD.  $\Delta[\theta]$  denotes the CD change at 205 nm after 24 h. (b) Inhibition of fibril formation examined by the ThT assay.

cence spectra of ThT were measured. EKEK alone showed a strong intensity when the structural transition to  $\beta$ -sheet was accomplished (Fig. 5). By contrast, intensities of ThT were extremely decreased when EKEK was incubated with cationic peptides (12.EKKK–16.KKKK) (Fig. 14b). These results imply that the cationic peptides had strong inhibition abilities for the amyloid formation as well as for the structural transition of EKEK, whereas the non-cationic peptides (2.EEEK–11.KKEE) were defective. The intensities of ThT were increased when EKEK was incubated with 6.EEKK, 10.KEKE or 11.KKEE, because these three peptides have the potential of amyloid formation in single species (Fig. 10). KKKK was most effective peptide in the inhibition and it inhibited the fibril formation of EKEK (12  $\mu$ M) at as low as 1  $\mu$ M concentration.<sup>66</sup>

The inhibition abilities of the cationic peptides were attributed to their high solubility to the water and to cationic repulsion between peptides. The cationic peptides may associate with EKEK with some affinity and increase the number of cationic charges and solubility of peptide complexes, thus inhibiting further assembling and the amyloid formation of peptides (Fig. 15). The fibril formation was not prevented when the inhibitors were added after the transition.

**3.3 Homologous Assembly and Inhibition.** KKKK and EKEK have homologous amino acid sequences except for the substitutions of four Lys residues for Glu residues in EKEK. To examine how a homologous peptide inhibits the amyloid formation, a series of peptides analogous to KKKK were designed and synthesized, such that the Ad groups were eliminated and replaced with acetyl groups or the sizes were

decreased to those of a single-chain and a half-length.<sup>66</sup> Inhibition abilities of KKKK analogous peptides for EKEK were evaluated by the ThT binding analyses. Consequently, the peptides with a higher homology to EKEK had a stronger inhibition ability. Ad- KKKK-2 $\alpha$  (KKKK) completely inhibited the amyloid formation of EKEK described above, and no fibrous structure was observed by TEM (Fig. 15). The two-stranded Ac-KKKK-2 $\alpha$  and the single-stranded Ad-KKKK-1 $\alpha$  also showed the strong inhibition ability, such that the fibrous structure was almost broken in TEM analyses. However, the short (half-length) peptides Ad- and Ac-KKKK-1/2 $\alpha$  had little inhibition ability. As a result, the cationic residues especially in the homologous sequences were important to inhibit the assembly and amyloid formation of EKEK.

Thus the inhibition of the amyloid formation of the model fibril peptide by cationic peptides with homologous sequences was accomplished, and the peptides with a higher homology to EKEK had a stronger inhibition ability. The finding that peptides with a homologous structure show the inhibition activity has some relevance to the fact that amyloidogenic peptides can assemble homogeneously by themselves and can show species-specificity in transmission of fibrils.<sup>1–4,9–12</sup> This new inhibition strategy focusing on the hydrophilic regions of peptides will give a useful insight for the therapeutic and diagnostic studies of amyloid diseases such as Alzheimer's and prion diseases. This kind of inhibition study is underway.

#### 4. Fabrication of Nanofibers with Uniform Morphology

Fabrication of nano-scale structures is one of the key goals in creating materials with extensive applications in nanotech-

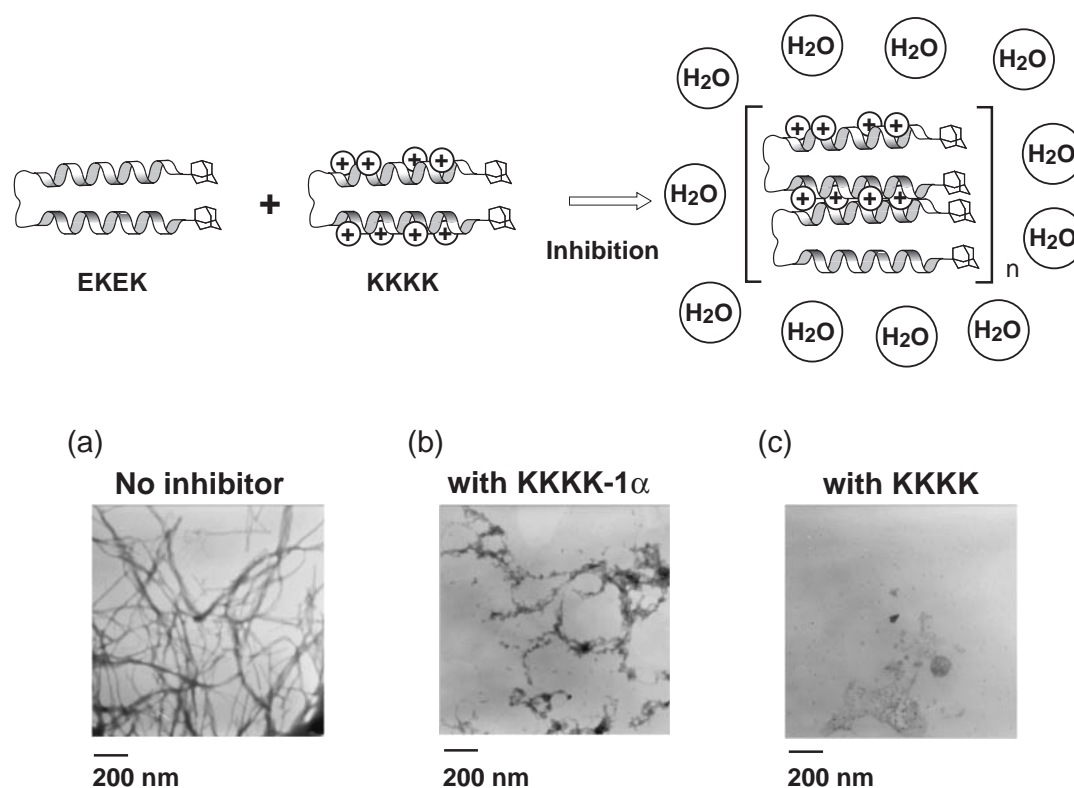


Fig. 15. Schematic representation of inhibition system by a homologous cationic peptide. The TEM images are shown; (a) EKEK alone without inhibitor, (b) EKEK with single strand KKKK-1 $\alpha$ , (c) EKEK with double strand KKKK.



nology. For nano-fabrication, molecular self-assembly is promising as a bottom-up approach. Natural organisms are rich in sophisticated materials built in a self-assembling manner, and materials with a natural basis are desired from ecological aspects. Many researchers have attempted to exploit the self-assembling properties of proteins and peptides for materials directed towards nano-devices, tissue engineering, and other applications.<sup>29–39,79–83</sup> In fibrous proteins and peptides mostly consisting of a  $\beta$ -sheet conformation, numerous  $\beta$ -strands are organized to form fibrous structures in a regular manner. Although  $\beta$ -sheet fibers are candidates for materials,<sup>29–39,79</sup> engineered  $\beta$ -sheet peptides generally tend to form aggregates with multiple morphologies such as bundled fibers or gels.<sup>45–56</sup> Typical sequences of designed  $\beta$ -sheet peptides have regular repeats of alternating hydrophobic and hydrophilic residues.<sup>40,45–50,84–86</sup> These sequences will make an amphiphilic binary pattern,<sup>84–86</sup> two distinct surfaces of hydrophobic and hydrophilic, in  $\beta$ -strands. The hydrophobic and complementary ionic interactions provide driving forces for the formation of  $\beta$ -strand assemblies together with hydrogen-bonding.<sup>45–56,59–64</sup> A variety of  $\beta$ -sheet peptides with an alternating hydrophobic and hydrophilic pattern were systematically designed, and the structures and gel formation behaviors were characterized in relation to the hydrophobic residues and ionic residues.<sup>45–50</sup> In order for researchers to exploit a single fiber and the alignment of  $\beta$ -strands within, as a nano-scale material, preventing gel formation and controlling the fiber morphology are important procedures. To this aim, artificial short peptides are advantageous because of the ease in strategic design of integrated or hybrid materials. We have developed the fabrication of controlled nanofibers through self-assembly of simple and short de novo designed  $\beta$ -sheet peptides with ten amino acid residues. As a result, homogeneous straight fibers with defined edges have been formed with a uniform morphology.<sup>68</sup>

**4.1 Peptide Design and Fiber Fabrication.** We designed amphiphilic  $\beta$ -sheet peptides composed of ten residues: Pro-Lys- $X_1$ -Lys- $X_2$ - $X_2$ -Glu- $X_1$ -Glu-Pro (Fig. 16).<sup>68</sup>  $X_1$  and  $X_2$  were hydrophobic residues selected from Phe, Ile, Val, or Tyr. Lys and Glu were utilized as hydrophilic residues. Many of de novo designed  $\beta$ -sheet peptides with a standard amphiphilic binary pattern easily aggregate to form bundles or gels of assembled peptides showing various morphologies. The broad hydrophobic or charged faces of  $\beta$ -strands can increase the possibility for varied arrangements of  $\beta$ -strands including

staggered arrangements. The hydrophobic and hydrophilic planes were divided to reduce such unfavorable possibility, and the order was inverted at the center of the strand. Additionally, the charged Lys and Glu residues were arranged to generate electrostatic attraction in an antiparallel strand orientation, but repulsion in a parallel orientation. Moreover, in order to cut the hydrogen-bonding network in the  $\beta$ -sheet structure at the strand ends, we employed Pro residues at both N- and C-termini. The Pro residue does not have an N-H available for hydrogen-bonding by virtue of the ring structure, and often acts as a  $\beta$ -sheet breaker.<sup>87</sup> Pro has an ability of reducing  $\beta$ -sheet expansion and extra fibril formation by stopping extension of the hydrogen-bonding network.<sup>88–90</sup> The above features potentially provided appropriate restrictions upon the assembly process, by regulating hydrophobic and hydrophilic interactions and hydrogen-bonding ability (Fig. 16). For fabrication of fibers, peptides were dissolved at a concentration of 50–200  $\mu$ M in 0.1 M sodium phosphate buffer (pH 7.4), and the solutions were allowed to stand at room temperature for more than a day.

**4.2 Fiber Morphology Studied by TEM and AFM.** For investigation of fiber morphology, TEM and atomic force microscopy (AFM) were utilized.<sup>68</sup> The peptide **FI** ( $X_1$  = Phe;  $X_2$  = Ile) formed homogeneous straight fibers, 80–130 nm in width and  $\sim$ 10  $\mu$ m in length with clear edges (Fig. 17). In the fine structure of the straight fiber, striations of about 10 nm width crossing each other were observed. Additionally, we observed fibers with a different morphology, namely a helical ribbon. In the ribbon, striations were also observed parallel to the ribbon edges. The helical ribbon appeared to densely coil and then grow to a straight fiber.

AFM images of the **FI** fibers resembled those visualized by TEM (Fig. 18). The **FI** fibers were 80–120 nm in width and had inner striations with 10–15 nm intervals. The height of straight fibers was 2–8 nm. The 3D-image of **FI** clearly showed a left-handed coiled ribbon. In the helical ribbons, the lower layer was 2–4 nm in height and the upper layer was 5–8 nm, approximately double that of the lower. These results strongly support the above idea that the straight fibers with clear edges were formed from tightly coiled ribbons.

This type of fiber was also formed from peptides other than **FI**. **IF** ( $X_1$  = Ile;  $X_2$  = Phe), **FV** ( $X_1$  = Phe;  $X_2$  = Val), and **VF** ( $X_1$  = Val;  $X_2$  = Phe) all formed helical ribbons and straight fibers with striations as successfully as **FI**. These peptides showed substantially the same morphologies as **FI** in respects of the straight fibers and coiled ribbons including the width. On the other hand, peptides with only aliphatic side chains in the hydrophobic residues showed fibers with a very different morphology. The peptides **VI** ( $X_1$  = Val;  $X_2$  = Ile), **IV** ( $X_1$  = Ile;  $X_2$  = Val), and **II** ( $X_1$  = Ile;  $X_2$  = Ile) formed straight fibers, but these appeared to have a tape-like morphology (Fig. 17). The tape-like fibers did not coil and were laterally associated into wider tapes of variable width (100–500 nm). No crossed striation was observed in these fibers. Thus, the peptides that formed helical ribbons and straight fibers with striations had hydrophobic aromatic Phe residues. Moreover, formation of straight fibers was supposedly attributed to the Pro residues at the both N- and C-termini, because 100 nm-size fibers with clear edges were not found in a peptide having Ala

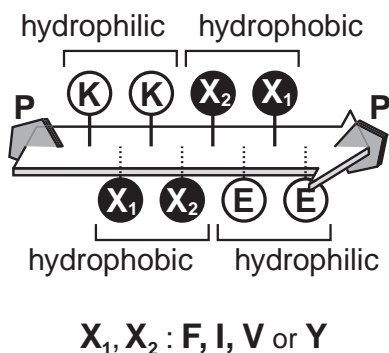


Fig. 16. Designed amphiphilic  $\beta$ -strand with terminal Pro residues for controlled fiber construction.



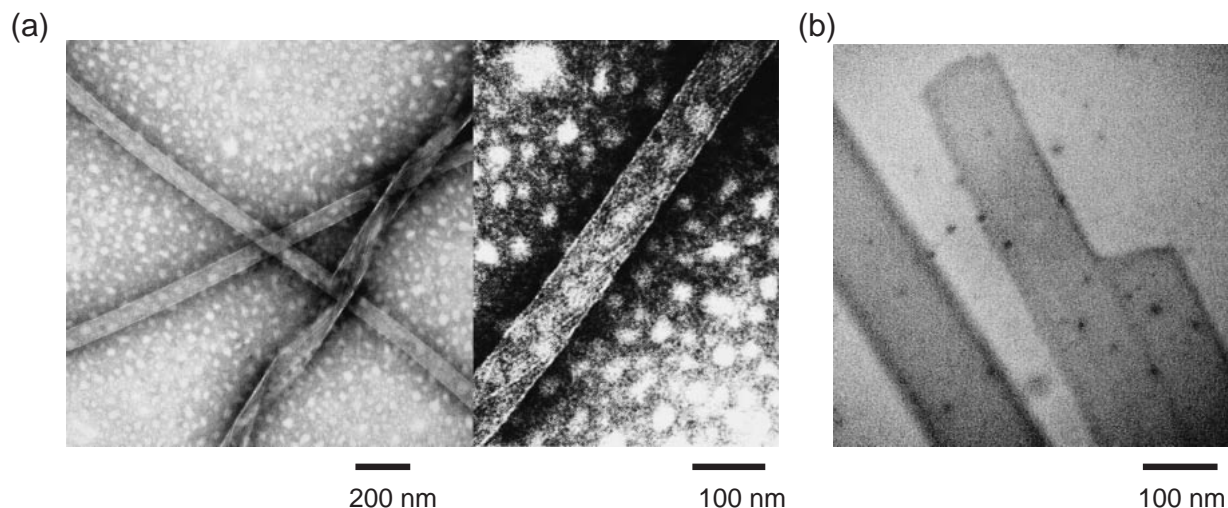


Fig. 17. TEM images of the coiled fibers self-assembled from FI (PKFKIIEFEP). (a) Both helical ribbon and straight fibers are shown (left). High magnification of the straight fiber shows crossed striations within (right). (b) TEM image of the tape-like fibers self-assembled from VI (PKVKIIEVEP).

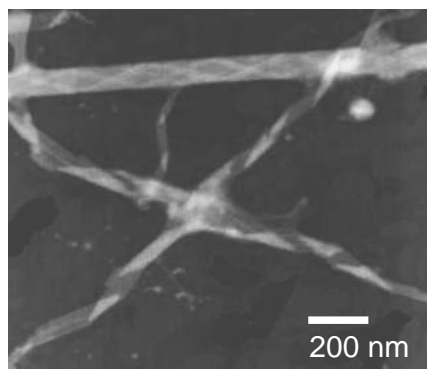


Fig. 18. Tapping-mode AFM image of the coiled fibers self-assembled from FI (PKFKIIEFEP).

residues at both termini. The Ala-containing peptide caused random aggregation of many small pieces of fiber. The Pro residues at both N- and C-termini contribute to controlled fiber formation.

**4.3 Hierarchical Fiber Formation.** The fibrous peptides and proteins self-assemble in a hierarchical manner (Fig. 19): peptide  $\beta$ -sheets assemble to form protofibrils, which associate into higher ordered fibrillar assemblies.<sup>9–12,54</sup> The reported protofibrils are 5–17 nm in width,<sup>9–12,26–28</sup> almost coincident with that of the striations in FI fibers (Fig. 17). This coincidence implies that protofibrils like those reported are initially formed from the peptide FI. The protofibrils align side-by-side to make up a ribbon, and then the ribbons helically coil to form straight fibers with 100 nm width. The straight fibers

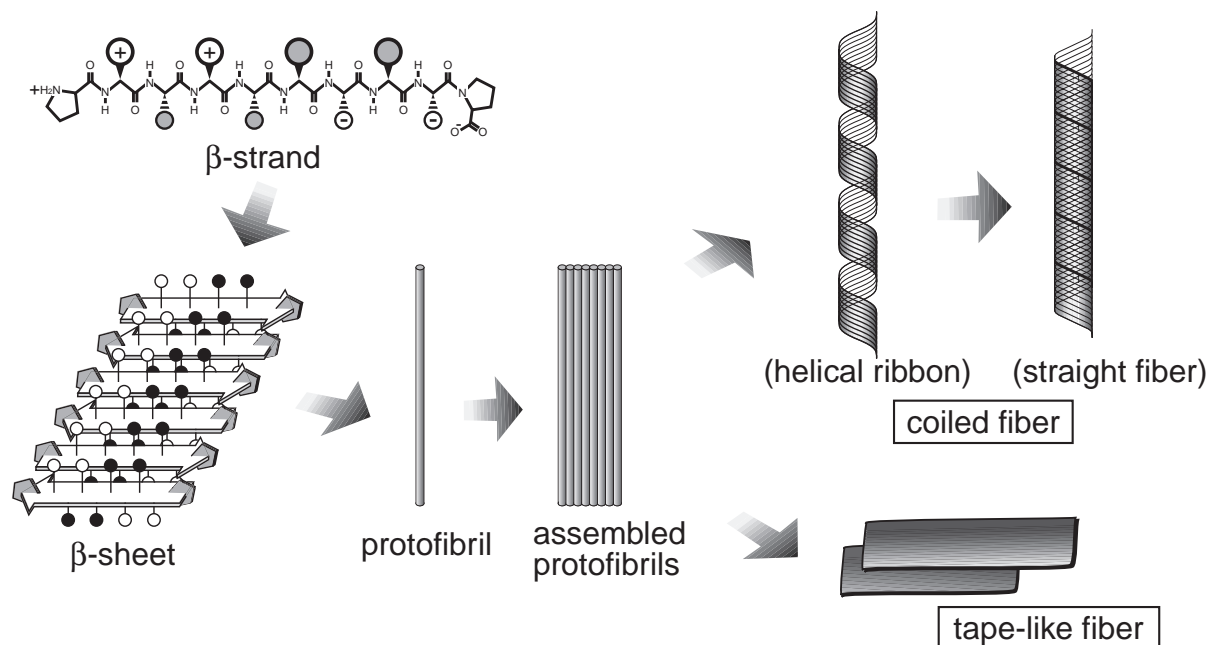


Fig. 19. Illustration of the hierarchical fiber formation self-assembled from ten-residue peptides (PKX<sub>1</sub>KX<sub>2</sub>X<sub>2</sub>EX<sub>1</sub>EP).

exist as a “single” fiber, and intertwining or bundling can be suppressed.

Fiber formation with uniform morphology would be contributed by the regular strand alignment. The strand alignment was enhanced by terminal Pro residues and the short length of the unique binary pattern. The order of hydrophilic and hydrophobic residues was reversed at the center of the strand. This pattern allowed both hydrophobic and hydrophilic interfaces on each side of a  $\beta$ -strand, and the narrow interfaces were capped by Pro residues incapable of hydrogen bonding. Pro residues ordered  $\beta$ -strands by aligning at the rim of  $\beta$ -sheets. Hydrophobic and electrostatic interactions on both sides of a  $\beta$ -sheet were available for precise recognition between the sheets, and the interactions work most effectively when the  $\beta$ -strands are in a regular unstaggered arrangement (Fig. 19). Electrostatic attractions are generated in antiparallel  $\beta$ -strand assemblies, and simultaneously aromatic interactions between Phe residues easily function. The recognition induces the strongly twisted  $\beta$ -sheet structure, which facilitates the formation of tightly coiled helical ribbons. Thereby, uniform straight fibers with clear edges are fabricated. Optimization of the interactions, including hydrogen-bonds, is advantageous for making defined  $\beta$ -sheet assemblies.

Fabrication of nano-scale fibers with homogeneous morphology was accomplished by self-assembly of designed  $\beta$ -sheet peptides. The peptides formed straight fibers with a uniform width and clear edges. The morphology could be controlled by peptide design: a unique amphiphilic binary pattern, Pro residues placed at both N- and C-termini, and a combination of

hydrophobic residues. Nanofibers with an ordered structure of self-assembled peptides can potentially be developed as biodegradable materials for applications in nanotechnology.

### 5. Construction of a Protein Array on Amyloid-Like Fibrils Using Co-assembly of Designed Peptides

We have previously demonstrated that de novo designed peptides undergo self-initiated structural transition and fibril formation, including representative properties of amyloid.<sup>59–64</sup> Cofibril formation from two, three, or four peptide species with well-designed amino acid sequences was achieved, so that the charged residues within the  $\beta$ -strands were complementary to each other.<sup>63,64</sup> This indicates a possibility of functionalizing the fibrils by co-assembling of peptides with various elements to develop a fibrillar peptide material as a well-ordered nano-construct (Fig. 20). As a step toward fabrication of a nanoscale array utilizing designed peptides, a protein (streptavidin) array immobilized onto fibrillar peptide assembly was produced.<sup>67</sup> The biotinylated peptides were incorporated into the fibrils co-assembled with non-biotinylated one, allowing regular immobilization of streptavidin onto the fibrils. The avidin-immobilized fibrils may make a nanoscaffold onto which a variety of functional groups can be arranged. The engineered fibrous peptides will be applied to develop arrays of chemical and biological molecules on the nanoscale construct.

**5.1 Co-assembly of Fibrils.** The new single-chained peptide  $\beta$ 16 and biotinylated B2x- $\beta$ 16 peptides<sup>67</sup> that could assemble into amyloid-like fibrils were designed according to the previous studies (Fig. 20).<sup>59–64</sup> B2x- $\beta$ 16 peptide had a bi-

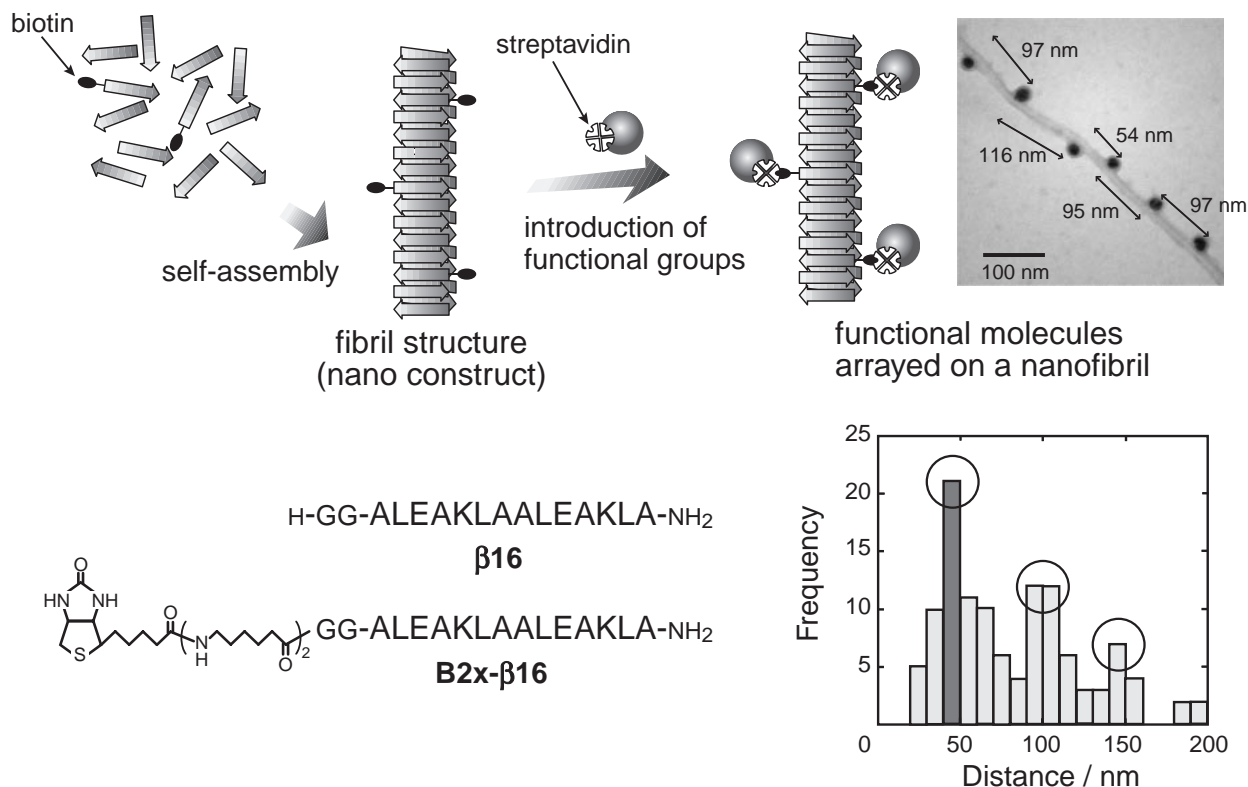


Fig. 20. Illustration of the cofibrils containing biotinylated peptides, and introduction of streptavidin with a functional group such as colloidal gold. TEM image shows arrayed gold particles on the cofibril of  $\beta$ 16/B2x- $\beta$ 16. Distances between gold particles and their frequency are indicated. Structures of  $\beta$ 16 and B2x- $\beta$ 16 are shown.

otin group at the N-terminus as a streptavidin-binding domain. Cofibril formation and its morphology of designed peptides were analyzed by CD measurement, ThT binding assay, and TEM analysis. Both  $\beta$ 16 alone and mixed peptides containing B2x- $\beta$ 16 formed a slightly  $\alpha$ -helical, but predominantly a random coil structure shortly after dilution in a buffer (pH 7.4). Through the incubation at 50 °C, transformation to  $\beta$ -sheet structure occurred time-dependently, supported by CD spectra with a negative peak at 219 nm and a positive peak at 203 nm. After the transition, ThT added to the peptide solutions exhibited strong fluorescence emission at 480 nm (excited at 440 nm). The result of ThT binding assay indicates that the  $\beta$ -structural peptides form amyloid-like fibrils. Direct observation of the peptide aggregates by TEM revealed that the peptides formed the fibrillar structures (Fig. 20). The fibrils were  $\sim$ 20 nm in width and of indeterminable length (several hundred nanometers to several micrometers).

**5.2 Protein Array on Fibrils.** Specific introduction of streptavidin onto the matured fibrils was achieved using co-assembling fibrils with biotinylated peptides.<sup>67</sup> One could pick out streptavidin under TEM observation if the streptavidin modified with colloidal gold (Au-Av: diameter of colloidal gold is 20 nm) was added onto the matured fibrils (1% B2x- $\beta$ 16). No Au-Av was observed on the fibrils formed by  $\beta$ 16 alone (containing no biotin), while attached Au-Av particles were observed on the fibrils containing B2x- $\beta$ 16 (Fig. 20). These results showed that biotinylated peptides were incorporated into fibrils, and that streptavidin molecules were attached to the biotin groups on the fibril.

The distance between successive Au-Av particles bound to the fibrils containing 1% B2x- $\beta$ 16 indicated that the gold particles were distributed preferably on average every 50, 100, and 150 nm (Fig. 20), suggesting a periodic binding of Au-Av particles on the fibrils at every ca. 50 nm. The distance of hydrogen-bonds between peptide strands is 4.7 Å along the fibril direction in cross- $\beta$ -sheet structure.<sup>9–12</sup> The average 50 nm intervals between Au-Av particles represent the distance for about 100–120 peptides aligned along the fibril axis. Hence, it can be ideally considered that one biotinylated peptide is preferably incorporated in every 100–120 peptides during fibrillogenesis. However, the observed fibrils with  $\sim$ 20 nm width are supposed to consist of several  $\beta$ -sheet filaments bundling regularly,<sup>9–12,54</sup> because the 5–6 nm-length peptide of  $\beta$ 16 (16 amino acid residues) makes a single filament of about 5 nm width. The assumed structure points out that distances between biotin groups along the fibril direction should be shorter than 50 nm, if biotinylated peptides were incorporated every 100 peptides. We have previously demonstrated using de novo designed peptides that the intermolecular side chain interactions such as ionic pairing, hydrogen bonding, and hydrophobic interaction were constitutive for the fibril formation.<sup>59–64,68</sup> The peptides used in this study were also well designed, considering the matching of the side chain interactions between antiparallel  $\beta$ -strands to regulate the fibril formation. Since the formed fibrils have a regularity or periodicity such as a helical ribbon in the fine structure, the biotin groups in the fibrils were exposed to aqueous environment according to the structural periodicity of fibrils determined by the side chain interactions, leading to the periodic binding of avidin onto the

fibrils. The biotinylated peptides were quantitatively and randomly incorporated into the cofibrils in a 1/100 content. Therefore, the frequency of bound Au-Av particles on the fibrils reflects the periodicity owing to the regular fibril structure. It is suggested that the arrangement of streptavidin on the peptide fibrils can be controlled using well-designed peptides.

The arrayed immobilization of natural protein onto the fibrillar nanoconstruct was successfully formed from designed peptides. Streptavidin was disposed regularly at every 50 nm interval on the fibrils containing biotinylated peptides. Other functional molecules can be arrayed onto the fibrils used in this study by adding functionalized streptavidin to biotinylated fibrils and/or adding functionalized biotin to streptavidin-immobilized fibrils. In fact, the fluorophore-labeled avidin bound to the fibrils has enabled the single fiber observation. Furthermore, engineered peptide fibrils formed from small peptides are of advantage, because the peptide element constructing fibrils can be easily modulated and modified by its amino acid composition, chain length, and incorporation of functional groups. The present study implies that a variety of functional molecules can be immobilized onto peptide nanofibrils in controlled distances and amounts, thus indicating the possibility to design nanoscale bioconstructs with functionalities.

## 6. Conclusions and Future Aspects

Conformational alternation and fibril formation of proteins have a key role in a variety of amyloid diseases including Alzheimer's and prion diseases. We have successfully developed peptides that undergo self-initiated structural transition from  $\alpha$ -helix to  $\beta$ -sheet and self-assembling into amyloid fibrils.<sup>59–65</sup> Peptides could be manipulated to assemble into amyloid fibrils in single and multiple (two, three, four) species.<sup>63,64</sup> These studies afforded the idea that homologous sequences of peptides have key roles in the  $\beta$ -sheet assembly and amyloid formation. This idea has been applied for design of the inhibition system of amyloid fibrils with homologous sequence assembly. Moreover, cofibril formation indicates a possibility of functionalizing the fibrils by co-assembling of peptides with various elements to develop a fibrillar peptide material as a well-ordered nanoconstruct. Another designing approach demonstrated the production of unique straight nanofibers with defined morphology. The fibrils may make a nanoscaffold onto which a variety of functional groups are arranged. The approaches accomplished in these studies are of advantage for designed and engineered peptides. The studies on engineering fibrous peptides will afford insight into disease-related amyloid formation and allow us to develop nanoscale fibrous constructs with further studies in nano and atomic level resolution. These materials with a natural basis developed by a self-assembling manner and a bottom-up approach are desired from ecological aspects for future soft-materials.

These studies are supported in part by the PRESTO and SORST programs of Japan Science and Technology Agency (JST) (HM), and grants from the Ministry of Education, Culture, Sports, Science and Technology (MEXT) (HM, TT). The authors thank students who have worked on these projects, especially Dr. Yuta Takahashi, who had developed the first stage of these designing studies of peptides.

## References

- 1 J. D. Sipe, *Annu. Rev. Biochem.*, **61**, 947 (1992).
- 2 J. W. Kelly, *Nat. Struct. Biol.*, **7**, 824 (2000).
- 3 J. W. Kelly, *Structure*, **5**, 595 (1997).
- 4 J. D. Harper, *Annu. Rev. Biochem.*, **66**, 385 (1997).
- 5 D. S. Selkoe, *Nature*, **426**, 900 (2003).
- 6 F. E. Cohen and J. W. Kelly, *Nature*, **426**, 905 (2003).
- 7 S. B. Prusiner, M. R. Scott, S. J. DeArmond, and F. E. Cohen, *Cell*, **93**, 337 (1998).
- 8 M. F. Tuite and B. S. Cox, *Nat. Rev. Mol. Cell Biol.*, **4**, 878 (2003).
- 9 O. S. Makin and L. C. Serpell, *Biochem. Soc. Trans.*, **30**, 521 (2002).
- 10 L. C. Serpell, *Biochim. Biophys. Acta*, **1502**, 16 (2000).
- 11 R. Tycko, *Curr. Opin. Struct. Biol.*, **14**, 96 (2004).
- 12 V. N. Uversky and A. L. Fink, *Biochim. Biophys. Acta*, **1698**, 131 (2004).
- 13 S. Ohnishi and K. Takano, *Cell. Mol. Life Sci.*, **61**, 511 (2004).
- 14 C. M. Dobson, *Nature*, **426**, 884 (2003).
- 15 M. Vendruscolo, J. Zurdo, C. E. MacPhee, and C. M. Dobson, *Philos. Trans. R. Soc. London, Ser. A*, **361**, 1205 (2003).
- 16 C. M. Dobson, *Philos. Trans. R. Soc. London, Ser. B*, **356**, 133 (2001).
- 17 C. M. Dobson, *Trends Biochem. Sci.*, **24**, 329 (1999).
- 18 H. Mihara and Y. Takahashi, *Curr. Opin. Struct. Biol.*, **7**, 501 (1997).
- 19 H. Mihara, Y. Takahashi, and A. Ueno, *Biopolymers*, **47**, 83 (1998).
- 20 S.-Y. Lin and H.-L. Chu, *Int. J. Biol. Macromol.*, **32**, 173 (2003).
- 21 K. Kuwata, M. Hoshino, S. Era, C. A. Batt, and Y. Goto, *J. Mol. Biol.*, **283**, 731 (1998).
- 22 K. Shiraki, K. Nishikawa, and Y. Goto, *J. Mol. Biol.*, **245**, 180 (1995).
- 23 D. L. Minor, Jr. and P. S. Kim, *Nature*, **380**, 730 (1996).
- 24 K.-M. Pan, M. Baldwin, J. Nguyen, M. Gasset, A. Serban, D. Groth, I. Mehlhorn, Z. Huang, R. J. Fletterick, F. E. Cohen, and S. B. Prusiner, *Proc. Natl. Acad. Sci. U.S.A.*, **90**, 10962 (1993).
- 25 T. R. Serio, A. G. Cashikar, A. S. Kowal, G. J. Sawicki, J. J. Moslehi, L. Serpell, M. F. Arnsdorf, and S. L. Lindquist, *Science*, **289**, 1317 (2000).
- 26 N. M. Kad, S. L. Myers, D. P. Smith, D. A. Smith, S. E. Radford, and N. H. Thomson, *J. Mol. Biol.*, **330**, 785 (2003).
- 27 C. Goldsbury, K. Goldie, J. Pellaud, J. Seelig, P. Frey, S. A. Müller, J. Kistler, G. J. S. Cooper, and U. Aebi, *J. Struct. Biol.*, **130**, 352 (2000).
- 28 T. S. Burkoth, T. L. S. Benzinger, V. Urban, D. M. Morgan, D. M. Gregory, P. Thiyagarajan, R. E. Botto, S. C. Meredith, and D. G. Lynn, *J. Am. Chem. Soc.*, **122**, 7883 (2000).
- 29 D. Hamada, I. Yanagihara, and K. Tsumoto, *Trends Biotechnol.*, **22**, 93 (2004).
- 30 S. Zhang, *Nat. Biotechnol.*, **21**, 1171 (2003).
- 31 S. S. Santoso, S. Vauthey, and S. Zhang, *Curr. Opin. Colloid Interface Sci.*, **7**, 262 (2002).
- 32 S. Zhang, D. M. Marini, W. Hwang, and S. Santoso, *Curr. Opin. Chem. Biol.*, **6**, 865 (2002).
- 33 S. H. Waterhouse and J. A. Gerrard, *Aust. J. Chem.*, **57**, 519 (2004).
- 34 M. Reches and E. Gazit, *Science*, **300**, 625 (2003).
- 35 J. E. Meegan, A. Aggeli, N. Boden, R. Brydson, A. P. Brown, L. Carrick, A. R. Brough, A. Hussain, and R. J. Ansell, *Adv. Funct. Mater.*, **14**, 31 (2004).
- 36 H. A. Lashuel, S. R. LaBrenz, L. Woo, L. C. Serpell, and J. W. Kelly, *J. Am. Chem. Soc.*, **122**, 5262 (2000).
- 37 C. E. MacPhee and C. M. Dobson, *J. Am. Chem. Soc.*, **122**, 12707 (2000).
- 38 T. Scheibel, R. Parthasarathy, G. Sawicki, X.-M. Lin, H. Jaeger, and S. L. Lindquist, *Proc. Natl. Acad. Sci. U.S.A.*, **100**, 4527 (2003).
- 39 "Self-Assembling Peptide Systems in Biology, Medicine and Engineering," ed by A. Aggeli, N. Boden, and S. Zhang, Kluwer Academic Publishers, Dordrecht (2001).
- 40 W. F. DeGrado, C. M. Summa, V. Pavone, F. Nastro, and A. Lombardi, *Annu. Rev. Biochem.*, **68**, 779 (1999).
- 41 W. D. Kohn and R. S. Hodges, *Trends Biotechnol.*, **16**, 379 (1998).
- 42 R. B. Hill, D. P. Raleigh, A. Lombardi, and W. F. DeGrado, *Acc. Chem. Res.*, **33**, 745 (2000).
- 43 M. L. de la Paz, K. Goldie, J. Zurdo, E. Lacroix, C. M. Dobson, A. Hoenger, and L. Serrano, *Proc. Natl. Acad. Sci. U.S.A.*, **99**, 16052 (2002).
- 44 R. A. Kammerer, D. Kostrewa, J. Zurdo, A. Detken, C. G.-Echeverria, J. D. Green, S. A. Müller, B. H. Meier, F. K. Winkler, C. M. Dobson, and M. O. Steinmetz, *Proc. Natl. Acad. Sci. U.S.A.*, **101**, 4435 (2004).
- 45 S. Zhang, "The Encyclopedia of Materials: Science & Technology," ed by K. H. J. Buschow, R. W. Cahn, M. C. Flemings, B. Ilschner, E. J. Kramer, and S. Mahajan, Elsevier Science, Oxford (2001), pp. 5822–5829.
- 46 Y. Hong, R. L. Legge, S. Zhang, and P. Chen, *Biomacromolecules*, **4**, 1433 (2003).
- 47 M. R. Caplan, E. M. Schwartzfarb, S. Zhang, R. D. Kamm, and D. A. Lauffenburger, *Biomaterials*, **23**, 219 (2002).
- 48 D. M. Marini, W. Hwang, D. A. Lauffenburger, S. Zhang, and R. D. Kamm, *Nano Lett.*, **2**, 295 (2002).
- 49 T. C. Holmes, S. de Lacalle, X. Su, G. Liu, A. Rich, and S. Zhang, *Proc. Natl. Acad. Sci. U.S.A.*, **97**, 6728 (2000).
- 50 M. Altman, P. Lee, A. Rich, and S. Zhang, *Protein Sci.*, **9**, 1095 (2000).
- 51 V. Kayser, D. A. Turton, A. Aggeli, A. Beevers, G. D. Reid, and G. S. Beddard, *J. Am. Chem. Soc.*, **126**, 336 (2004).
- 52 A. Aggeli, M. Bell, N. Boden, L. M. Carrick, and A. E. Strong, *Angew. Chem., Int. Ed.*, **42**, 5603 (2003).
- 53 A. Aggeli, M. Bell, L. M. Carrick, C. W. G. Fishwick, R. Harding, P. J. Mawer, S. E. Radford, A. E. Strong, and N. Boden, *J. Am. Chem. Soc.*, **125**, 9619 (2003).
- 54 A. Aggeli, I. A. Nyrkova, M. Bell, R. Harding, L. Carrick, T. C. B. McLeish, A. N. Semenov, and N. Boden, *Proc. Natl. Acad. Sci. U.S.A.*, **98**, 11857 (2001).
- 55 C. W. G. Fishwick, A. J. Beevers, L. M. Carrick, C. D. Whitehouse, A. Aggeli, and N. Boden, *Nano Lett.*, **3**, 1475 (2003).
- 56 A. Aggeli, M. Bell, N. Boden, J. N. Keen, P. F. Knowles, T. C. B. McLeish, M. Pitkeathly, and S. E. Radford, *Nature*, **386**, 259 (1997).
- 57 S. Zhang, L. Yan, M. Altman, M. Lässle, H. Nugent, F. Frankel, D. A. Lauffenburger, G. M. Whitesides, and A. Rich, *Biomaterials*, **20**, 1213 (1999).
- 58 J. Kisiday, M. Jin, B. Kurz, H. Hung, C. Semino, S. Zhang, and A. J. Grodzinsky, *Proc. Natl. Acad. Sci. U.S.A.*, **99**, 9996 (2002).
- 59 Y. Takahashi, A. Ueno, and H. Mihara, *Chem.—Eur. J.*, **4**, 2475 (1998).



- 60 Y. Takahashi, A. Ueno, and H. Mihara, *Bioorg. Med. Chem.*, **7**, 177 (1999).
- 61 Y. Takahashi, T. Yamashita, A. Ueno, and H. Mihara, *Tetrahedron*, **56**, 7011 (2000).
- 62 Y. Takahashi, A. Ueno, and H. Mihara, *Structure*, **8**, 915 (2000).
- 63 Y. Takahashi, A. Ueno, and H. Mihara, *ChemBioChem*, **1**, 75 (2001).
- 64 Y. Takahashi, A. Ueno, and H. Mihara, *ChemBioChem*, **3**, 637 (2002).
- 65 Y. Takahashi and H. Mihara, *Bioorg. Med. Chem.*, **12**, 693 (2004).
- 66 T. Yamashita, Y. Takahashi, T. Takahashi, and H. Mihara, *Bioorg. Med. Chem. Lett.*, **13**, 4051 (2003).
- 67 H. Kodama, S. Matsumura, T. Yamashita, and H. Mihara, *Chem. Commun.*, **2004**, 2876.
- 68 S. Matsumura, S. Uemura, and H. Mihara, *Chem.—Eur. J.*, **10**, 2789 (2004).
- 69 S. Matsumura, S. Sakamoto, A. Ueno, and H. Mihara, *Chem.—Eur. J.*, **6**, 1781 (2000).
- 70 D. Yana, T. Takahashi, H. Mihara, and A. Ueno, *Macromol. Rapid Commun.*, **25**, 577 (2004).
- 71 T. Morii, J. Yamane, Y. Aizawa, K. Makino, and Y. Sugiura, *J. Am. Chem. Soc.*, **118**, 10011 (1996).
- 72 W. C. Chan and P. D. White, "Fmoc Solid Phase Peptide Synthesis," ed by W. C. Chan and P. D. White, Oxford University Press, New York (2000), pp. 41–76.
- 73 H. LeVine, III, *Methods Enzymol.*, **309**, 274 (1999).
- 74 W. E. Klunk, R. F. Jacob, and R. P. Mason, *Anal. Biochem.*, **266**, 66 (1999).
- 75 M. A. Findeis, *Biochim. Biophys. Acta*, **1502**, 76 (2000).
- 76 L. O. Tjernberg, J. Näslund, F. Lindqvist, J. Johansson, A. R. Karlström, J. Thyberg, L. Terenius, and C. Nordstedt, *J. Biol. Chem.*, **271**, 8545 (1996).
- 77 L. O. Tjernberg, C. Lilliehöök, D. J. E. Callaway, J. Näslund, S. Hahne, J. Thyberg, L. Terenius, and C. Nordstedt, *J. Biol. Chem.*, **272**, 12601 (1997).
- 78 L. A. Scrocchi, Y. Chen, S. Waschuk, F. Wang, S. Cheung, A. A. Darabie, J. McLaurin, and P. E. Fraser, *J. Mol. Biol.*, **318**, 697 (2002).
- 79 J. D. Hartgerink, E. Beniash, and S. I. Stupp, *Science*, **294**, 1684 (2001).
- 80 Z. Li, S.-W. Chung, J.-M. Nam, D. S. Ginger, and C. A. Mirkin, *Angew. Chem., Int. Ed.*, **42**, 2306 (2003).
- 81 M. Knez, A. M. Bittner, F. Boes, C. Wege, H. Jeske, E. Maiß, and K. Kern, *Nano Lett.*, **3**, 1079 (2003).
- 82 R. A. Mcmillan, C. D. Paavola, J. Howard, S. L. Chan, N. J. Zaluzec, and J. D. Trent, *Nat. Mater.*, **1**, 247 (2002).
- 83 M. G. Ryadnov, B. Ceyhan, C. M. Niemeyer, and D. N. Woolfson, *J. Am. Chem. Soc.*, **125**, 9388 (2003).
- 84 M. W. West and M. H. Hecht, *Protein Sci.*, **4**, 2032 (1995).
- 85 M. W. West, W. Wang, J. Patterson, J. D. Mancias, J. R. Beasley, and M. H. Hecht, *Proc. Natl. Acad. Sci. U.S.A.*, **96**, 11211 (1999).
- 86 G. Xu, W. Wang, J. T. Groves, and M. H. Hecht, *Proc. Natl. Acad. Sci. U.S.A.*, **98**, 3652 (2001).
- 87 P. Y. Chou and G. D. Fasman, *Annu. Rev. Biochem.*, **47**, 251 (1978).
- 88 D. F. Moriarty and D. P. Raleigh, *Biochemistry*, **38**, 1811 (1999).
- 89 D. T. S. Rijkers, J. W. M. Höppener, G. Posthuma, C. J. M. Lips, and R. M. J. Liskamp, *Chem.—Eur. J.*, **8**, 4285 (2002).
- 90 H. Rapaport, K. Kjaer, T. R. Jensen, L. Leiserowitz, and D. A. Tirrell, *J. Am. Chem. Soc.*, **122**, 12523 (2000).



Hisakazu Mihara was born in Yamaguchi in 1958. He received his B.S. degree in 1981, M.S. in 1983, Dr.Sc. in Chemistry in 1986 at Kyushu University under the supervision of Professor Nobuo Izumiya. He was a postdoctoral fellow in Professor Emil T. Kaiser laboratory at the Rockefeller University from 1986. He was appointed as an Assistant Professor at Kyushu Institute of Technology in 1988, and promoted to an Associate Professor at Nagasaki University in 1993. Currently, he has been involved in the Department of Bioengineering, Tokyo Institute of Technology, as an Associate Professor from 1995, and a researcher in the national project of PRESTO & SORST program of Japan Science and Technology Agency from 1998. His research interests include peptide design and synthesis, and peptide engineering such as fibrous peptides and peptide microarrays.



Sachiko Matsumura was born in Gumma in 1974. She received her B.S. degree in 1997, M.S. in 1999, and Dr.Eng. in 2002 at Tokyo Institute of Technology under the supervision of Associate Professor Hisakazu Mihara. At present, she belongs to the Corporate Research Laboratory, Fuji Xerox Co., Ltd. as a postdoctoral fellow from 2002. Her current research concerns the peptide design and synthesis for the fabrication of peptide nanostructures and materials.





Tsuyoshi Takahashi was born in Kanagawa in 1972. He received his B.S. degree in 1996, M.S. in 1998, and Dr.Eng. in 2001 at Tokyo Institute of Technology under the supervision of Associate Professor Hisakazu Mihara. He was a research fellow of the Japan Society for the Promotion of Science (JSPS) for Young Scientist from 2000. At present he is an Assistant Professor at Tokyo Institute of Technology from 2002. His current research interests are de novo design of peptides and proteins with 3D structures, and construction of RNA molecules that bind to amyloid peptides and inhibit the amyloid fibril formation.